Analysis of the eastern Adriatic sea-level extremes

Pervan, Marija

University of Split
Faculty of Science

ANALYSIS OF THE EASTERN ADRIATIC SEA-LEVEL EXTREMES

Master thesis

Marija Pervan

Split, July 2021

Zahvaljujem svojoj mentorici doc. dr. sc. Jadranki Šepić na dragocjenim savjetima, potpori, prenesenom znanju i strpljenju, ne samo prilikom izrade diplomskog rada, nego i za vrijeme cijelog diplomskog studija. Uvijek ću biti zahvalna na prilici za rad s Vama i za učenje od Vas.

Hvala i svim profesorima kroz ovih 5 godina studiranja. Hvala na prenesenom znanju, hvala za radost odlaska na predavnja i hvala što se nam pokazali što znači biti fizičar i s ljubavlju raditi svoj posao.

Hvala svim prijateljima i kolegama.

Puno hvala mojoj obitelji. Bez vas i vaše podrške, motivacije i ljubavi ovo ne bi bilo moguće.

I za kraj, hvala mom suprugu. Tome, hvala što si bio moj oslonac sve ove godine. Hvala na strpljenju, podršci i ljubavi. Hvala što si vjerovao da ja to mogu.

Temeljna dokumentacijska kartica

Sveučilište u Splitu
Prirodoslovno – matematički fakultet
Odjel za fiziku
Ruđera Boškovića 33, 21000 Split, Hrvatska

Diplomski rad

Analiza ekstremnih razina mora na području istočnog Jadrana

Marija Pervan

Sveučilišni diplomski studij Fizika, smjer Fizika okoliša

Sažetak:
Područje Jadranskog mora često pogađaju poplave uzrokovane olujnim usporima i meteotsunamijima. U lipnju 2017. godine u Starom Gradu (otok Hvar; središnji Jadran) postavljen je mareograf s minutnom rezolucijom mjerenja. Analizirane su tri godine mjerenja razine mora te je izdvojeno 10 najjačih epizoda od svakog tipa ekstremnih razina mora: (1) pozitivni dugo-periodički ($T > 210$ min) ekstremi; (2) negativni dugo-periodički ($T > 210$ min) ekstremi; (3) kratko-periodički ($T < 210$) ekstremi. Podaci ERA5 reanalize pokazali su da se pozitivni dugo-periodički ekstremi javljaju za vrijeme prisutnosti niskog tlaka zraka nad Jadranom, te puhanja izraženog jugoistočnog vjetra (*jugo*). Negativni dugo-periodički ekstremi javljaju se za vrijeme prisutnosti polja visokog tlaka zraka nad Jadranom te puhanja jakih vjetrova sa sjeveroistoka (*bura*) ili za mirna vremena bez vjetra. S druge strane, kratko-periodički ekstremi javljaju se i za lošeg vremena (nizak tlak, snažni jugoistočni vjetar) i za mirna, lijepa vremena (normalan/visok tlak, bez vjetra).

Ključne riječi: razina mora, Jadransko more, ekstremi, meteotsunami, olujni uspor

Rad sadrži: 38 stranica, 39 slika, 4 tablice, 18 literaturnih navoda. Izvornik je na engleskom jeziku

Mentor: doc. dr. sc. Jadranka Šepić

Ocjenjivači: doc. dr. sc. Jadranka Šepić
doc. dr. sc. Žarko Kovač
dr. sc. Marin Vojković

Rad prihvaćen: 14. 7. 2021.

Rad je pohranjen u knjižnici Prirodoslovno – matematičkog fakulteta, Sveučilišta u Splitu.

Basic documentation card

University of Split
Faculty of Science
Department of Physics
Ruđera Boškovića 33, 21000 Split, Croatia

Master thesis

Analysis of the eastern Adriatic sea-level extremes

Marija Pervan

University graduate study programme Physics, orientation Environmental Physics

Abstract:
The Adriatic Sea is known to be under a high flooding risk. In June 2017, a tide-gauge station with a 1-min sampling resolution has been installed at Stari Grad (Hvar Island, middle Adriatic Sea). Three years of corresponding sea-level measurements were analyzed, and 10 strongest episodes of each of the following extreme types were extracted: positive long-period (T > 210 min) extremes; negative long-period (T > 210 min) extremes; short-period (T < 210) extremes. It was shown that positive low-pass extremes commonly appear during the presence of low pressure over the Adriatic associated with strong SE winds (*sirocco*). Negative low-pass extremes are associated with the high atmospheric pressure over the area associated with either strong NE winds (*bora*), or no winds at all. On the other hand, high-pass sea level extremes are observed during two types of atmospheric situations corresponding to both "bad" (low pressure, strong SE wind) and "nice" (normal/high pressure, no wind) weather.

Keywords: sea level, the Adriatic Sea, extremes, meteotsunami, storm surge

Thesis consists of: 38 pages, 39 figures, 4 tables, 18 references. Original language: English

Supervisor: Assist. Prof. Dr. Jadranka Šepić

Reviewers: Assist. Prof. Dr. Jadranka Šepić
Assist. Prof. Dr. Žarko Kovač
Dr. Marin Vojković

Thesis accepted: July 14, 2021.

Thesis is deposited in the library of the Faculty of Science, University of Split.

Content

1 Introduction

One of the most threatening effects of climate change is the anticipated sea-level rise which can generate significant damage to coastal regions. For example, Venice – an important Italian port, tourist and cultural centre, is often hit by a widely recognized phenomenon called *aqua alta*, extreme flood that lasts for hours. Not only Venice is vulnerable to the effects of climate change and extreme sea levels, but also majority of the Adriatic cost. Croatian islands are often affected by sea-level phenomena leading to floods such as storm surges, seiches and meteotsunamies. Additionally, tides play an important role in driving sea-level extremes in the Adriatic Sea, being large in comparison with the tides occuring in other parts of the Mediterrenean. Occasionally, high atmospheric pressure along with the bora wind can generate negative sea-level extremes. The research of these effects can help mitigate the hazards and deepen the understanding of Adriatic, by developing and implementing warning systems for the populated areas. [1]

The Adriatic Sea is a marginal Mediterranean sea of a bay-like shape, it has length of 800 km and width of around 200 km. It is positioned between coastlines of Italy, Slovenia, Croatia, Bosnia and Herzegovina, Montenegro and Albania. The Adriatic Sea has a surface of ~138.600 km^2 and a volume of ~35000 km^3. Depth of the Adriatic Sea increases going from the north to the south, with an average depth of 35 m in the northern Adriatic, 150 m in the central Adriatic and 450 in the southern Adriatic (Figure 1). Deepest part of the middle Adriatic is Jabuka Pit with depths reaching 270 m, and deepest part of the south Adriatic is the South Adriatic Pit with depths reaching 1200 m. The eastern Adriatic coastline is indented and has many islands unlike the western Adriatic coastline (Figure 1). [2]

In the Adriatic Sea, extreme sea levels occur due to the following processes [1]: (1) sea-level rise induced by climate change; (2) seasonal sea-level changes and interanuall variability; (3) response to planetary-scale atmospheric forcing; (4) storm surges; (5) basin-wide seiches; (6) tides, and (7) high-frequency phenomena. A superposition of these processes can happen, resulting in hazardous events, in particular floods.

The thesis is organized as follows: Introduction is given in the first chapter; extended introduction into processes resulting in sea-level extremes is in the second chapter; materials and methods are described in the third chapter; results are presented in the fourth chapter, and conclusions and discussion are in the fifth chapter.

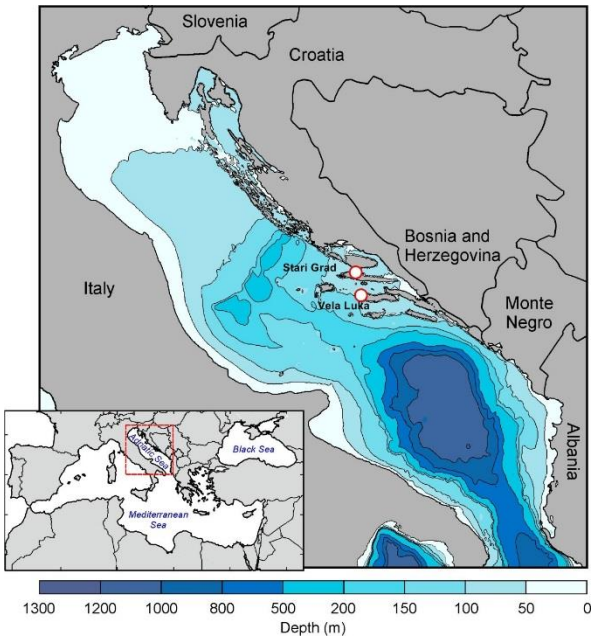

Figure 1. *Position and bathymetry of the Adriatic Sea with indicated tide gauges at Vela Luka and Stari Grad.*

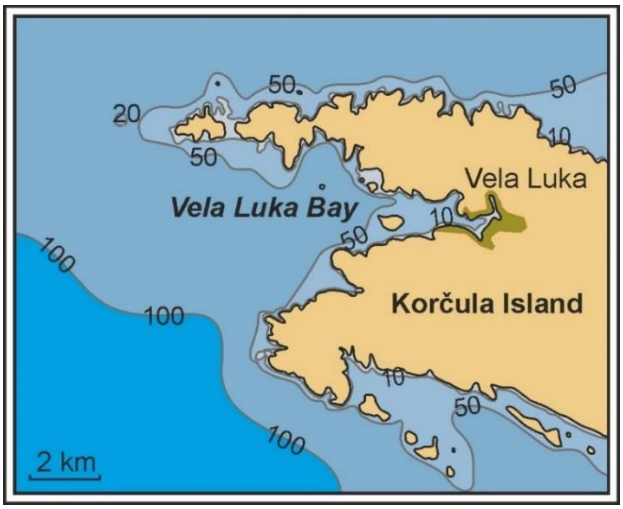

Figure 2. *Bathymetry of Vela Luka Bay, source [3].*

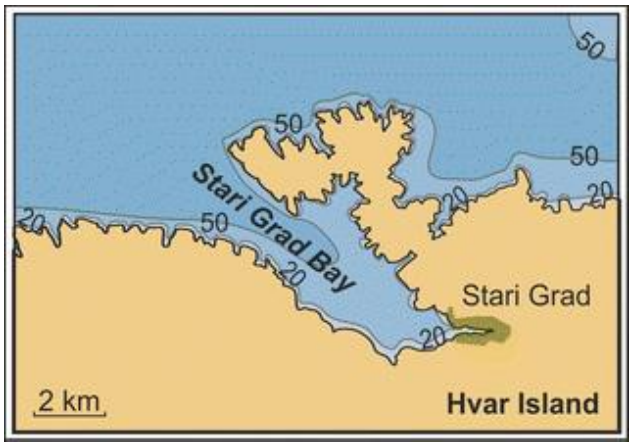

Figure 3. *Bathymetry of Stari Grad Bay, source [3].*

2 Processes resulting in sea-level extremes in the Adriatic

2.1 Sea-level rise induced by climate change

Sea level has been rising during the last 2000 years at least – firstly, the sea level rose during deglaciation, increasing the mean sea level for ~1.5 m. [4] Today, global sea-level rise is mostly due to antropohogenically induced global warming resulting with the the ice melting, as well as thermal expansion of seawater. The expected worldwide sea-level rise by the year 2100 is 26-55 cm (RCP2.6 scenario), 32-63 cm (RCP4.5 scenario) or 45-82 cm (RCP8.5). [5]

2.2 Seasonal sea-level changes and interannual variability

Seasonal sea-level changes happen due to air pressure changes, wind effects, influence of heat flux and pumping of fresh water. [1] Barotropic model driven by air pressure and wind forcing shows was used and it was shown that the Adriatic sea level has seasonal and semi-seasonal cycle. Annual cycle maximum occurs in March or April and maxima of the semiannual cycle occur in January/February and July/August. Moreover, the Adriatic Sea sea-level anomalies are strongly related to the air pressure anomalies that occur simultaneously. A 1 mbar increase/decrease of air pressure corresponds to a 1.8-2.0 cm lowering/rising of the sea level. The Mediterranean Sea level anomalies are typically of a barotropic nature. Many authors found a correlation between interannual sea-level variability and the NAO (North Atlantic Oscillation) – the NAO influence on the Adriatic Sea sea levels is mostly associated to the air pressure and wind forcing. [1]

2.3 Response to planetary-scale atmospheric forcing

Sea-level changes at time scales between 10 days and a couple of months are induced by the slow air pressure variations and winds. [1] These winds are related to the passage of planetary atmospheric waves over the sea, and best observed in the middle troposphere. Sea-level changes on these time scales account for around one third of the Adriatic sea-level variability. Furthermore, they are especially energetic in winter (amplitudes can surpass 30 cm) with larger amplitudes in the northern parts of the Adriatic Sea than the southern. However, sea-level changes related to the planetary-scale forcing show a faintly negative trend in the Adriatic over the last fifty years. [1]

2.4 Storm surges

The strongest flood events in the Adriatic Sea happen during storm surges. [1] Storm surges are short-lived sea-level increases which occur due to synoptic-scale air pressure and wind forcing. In the Adriatic they mostly occur when a low atmospheric pressure (cyclone) over the Gulf of Genoa is conjoined with the strong sirocco winds (*jugo*) blowing along the Adriatic Sea. These south-eastern winds can push water mass for hours or days towards the northern

parts of the Adriatic Sea resulting in floods. These floods are frequent in Venice – *acqua alta* (Figure 4), but can also happen on the eastern coast of the Adriatic. Occurrence of storm surges in the future will be governed by the changes of the cyclone activity over the Adriatic and by the future mean sea-level changes. Even tough the projections show a decrease in the frequency and intensity of cyclones over the Mediterranean, the trend in the magnitude of annual sea-level maxima in the Adriatic is expected to be positive in the second half of the twenty-first century due to sea-level rise. It is worth mentioning that negative storm surges can happen during high atmospheric pressure and bora winds in the Adriatic. North-eastern winds push water mass from the Croatian coast to the Italian cost. Along with the high pressure, this phenomenon can lower sea level on the east coast of the Adriatic over 30 cm. [1], [6]

2.5 Basin-wide seiches

When a sirocco wind stops, related storm surge relaxes through a series of oscillations which form a standing wave called seiche. [1] Seiches occur in lakes, harbors, bays and partially enclosed seas such as the Adriatic Sea. The period of the Adriatic Sea's fundamental mode is ~21.2 h. This mode accounts for ~2-3% of the total Adriatic sea-level variance. Periods of the two following modes are at ~10.7 hours and ~6.7 hours. Decay time of the Adriatic seiche is estimated to be around 3.2 days. Energy leakage is caused by frictional effects and the open boundary – the Otranto Strait. Interestingly, there has been a gradual decrease of fundamental seiche period in analyses over the years (from 23 to 22 hours, to 21.2 hours). It is not clear whether this uncertanty is due to the improvement of methods of analysis or is this a physical phenomenon. It is possible that the wide range of fundamental periods comes from different approaches to the open boundary condition. [1]

Figure 4. *Acqua alta in Venice in November 2019, source [7].*

2.6 Tides

Tides are regular changes in the sea level caused by the gravitational attraction of the Moon and the Sun along with the Earth-Moon and Earth-Sun rotations. The Adriatic tides can be well approximated by four semidiurnal (M_2, S_2, N_2 and K_2) and three diurnal (K_1, O_1, P_1) harmonic constituents. Semidiurnal tides have an amphidromic point halfway between Šibenik and Ancona. They grow in amplitudes towards the north Adriatic and also have secondary maxima along the Palagruža Sill. Diurnal tides rise in amplitudes from the southern to the northern parts of the Adriatic (Figure 5). As a result, tidal range in the southern parts of the Adriatic is approximatelly 30 cm and in the Gulf of Trieste it is approximatelly 120 cm. [1], [8]

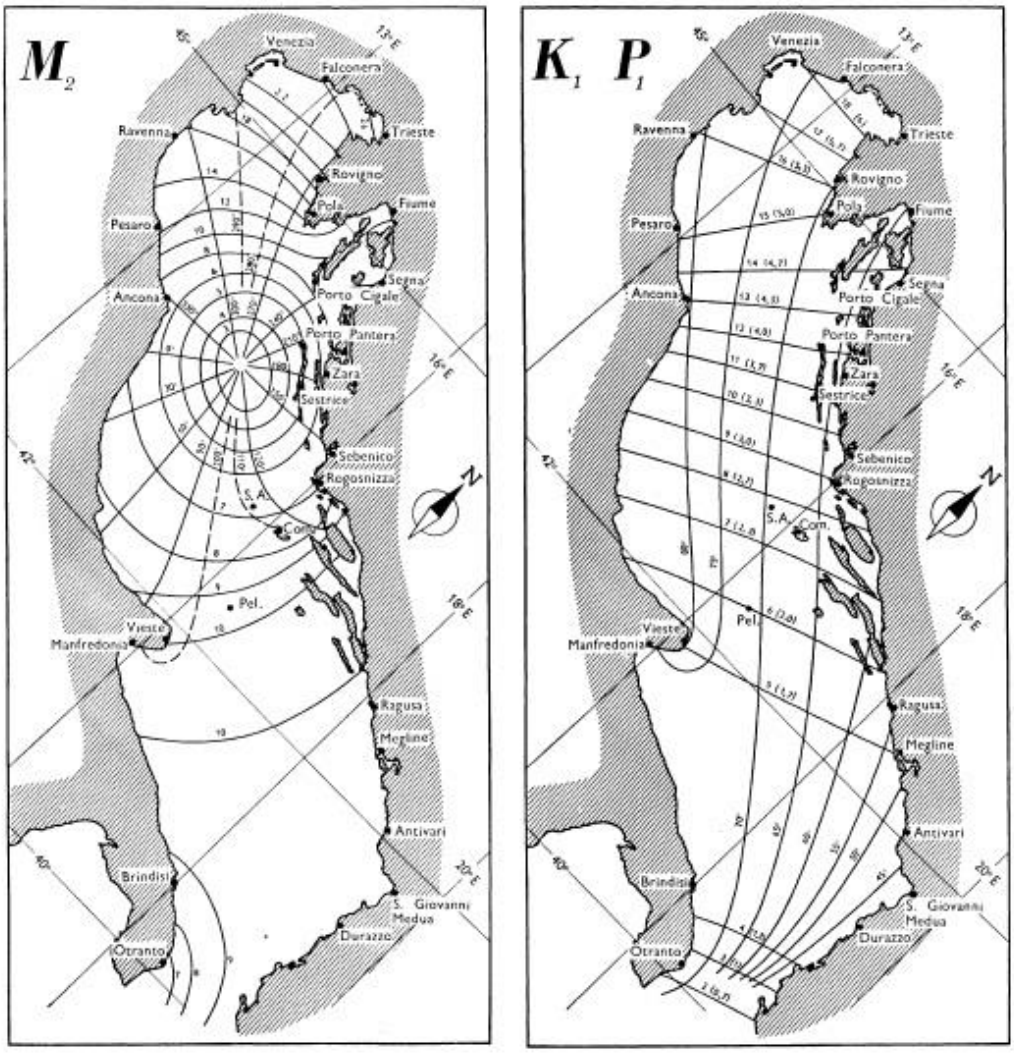

Figure 5. *Semidiurnal (left) and diurnal (right) tidal constituents in the Adriatic Sea, source [9].*

2.7 High-frequency phenomena

2.7.1 Local seiches

High-frequency phenomena causing sea-level extremes in the Adriatic are local seiches, seismic and landslide tsunamis and meteotsunamis. Local seiches are driven by long ocean

waves advancing towards a bay, e.g. Vela Luka seiche (Figure 2) or Stari Grad seiche (Figure 3). Direct forcing is typically not capable of generating major oscillations in small basins. Studies on the local seiches for several Adriatic harbours have been conducted. For example, it was shown that Ploče Harbour has fundamental period of 30 minutes, with a number of other significant modes (4.1 h, 2.6 h and 1.5 h), and Bakar Bay, e.g., has a wide energy peak between 19 and 27 minutes. [1]

2.7.2 Tsunamis

The Adriatic Sea has lower seismic and tsunamigenic capacity than some other parts of the Mediterranean. However, a couple of destructive tsunamis have occurred in the past. [1] The most researched tsunami in the Adriatic Sea is the Gargano tsunami of 1627. Together with the earthquake that triggered it, it claimed 4000 lives. The most recent one was in 1979 after the Montegrin earthquake. Hazard scenarios for seismic tsunamis were developed, and the strongest one, with maximum wave amplitude of 5 m, is modelled at Dubrovnik. [1]

2.7.3 Meteotsunamis

Often, meteotsunamis are mistaken for tsunamis. [10] They affect coastal regions in a similarly destructive way as tsunamis, but they are generated by atmospheric pressure disturbances and not by underwater earthquakes, landslides and volcanic explosions. The Adriatic Sea is considered a meteotsunami *hot spot.* The strongest meteotsunami on record happened in Vela Luka in 1978 (Figure 6). Vela Luka was hit by a series of destructive waves with heights up to 6 m. In 2003, a meteotsunami with 3-m high waves hit Stari Grad on Hvar island. Even though many more destructive meteotsunamis struck Adriatic coast [11], there are no meteotsunamis warnings currently available for the Adriatic. In the Mediterranean, meteotsunami warnings are now available only for the area of the Balearic Islands. [1]

Figure 6. *Meteotsunami in Vela Luka, 1978, source [12].*

All of the above-listed processes seem to be relevant for two middle Adriatic harbours, Vela Luka (Korčula Island) and Stari Grad (Hvar Island), for which 1-min sea level and meteorological measurements have been available at least since July 2017. After initial analysis, We have discovered that there is a lack of data from the Vela Luka, limiting the quality of the proposed research. Therefore, in this thesis I focus on studying the Stari Grad bay sea-level extremes. Stari Grad bay, as well as Vela Luka bay, has a complex bathymetry (Figure 3) and it experiences pronounced local seiches. Additionally, meteotsunamis were also documented there. [11] Lastly, being situated on the island in the central Adriatic, Stari Grad bay and Vela Luka bay can face sea-level extremes due to storm surges as well.

3 Materials and methods

3.1 Materials

Oceanographic and atmospheric data used in this thesis were measured at automatic measuring stations located in Stari Grad (Island Hvar) and operated by the Institute of Oceanography and Fisheries, Split, Croatia. [13] I analyzed one minute time series of air temperature, air pressure, wind speed, wind direction and sea level, measured in a period 28th June 2017 - 5th August 2020 (Figure 7, Figure 8, Figure 9, and Figure 10). For the analysis of synoptic conditions the ERA5 reanalysis data were used. [14] All analyses were done in Matlab R2020a.

3.2 Methods

3.2.1 Data quality analysis

As a first step of data analysis, all data was quality checked. In total, only 391 sea-level data points (~6.5 hours), 33 wind speed and direction data points and 38 air pressure data points of three years of 1-min data were missing, and the remaining data was of high quality. The gaps were filled using linear interpolation (MATLAB *interp1* function).

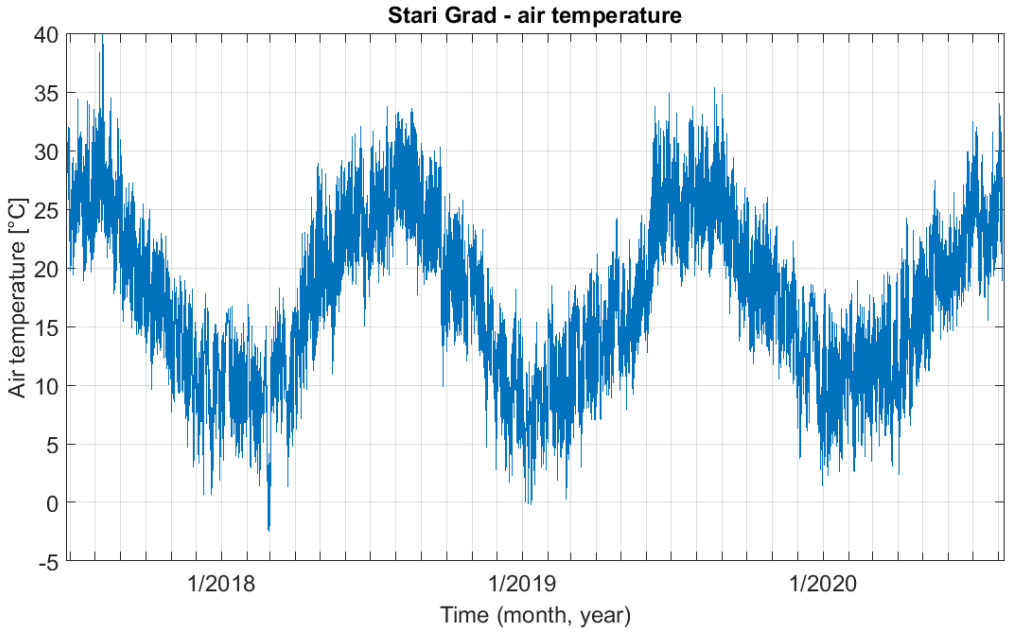

Figure 7*. Interpolated air temperature time series.*

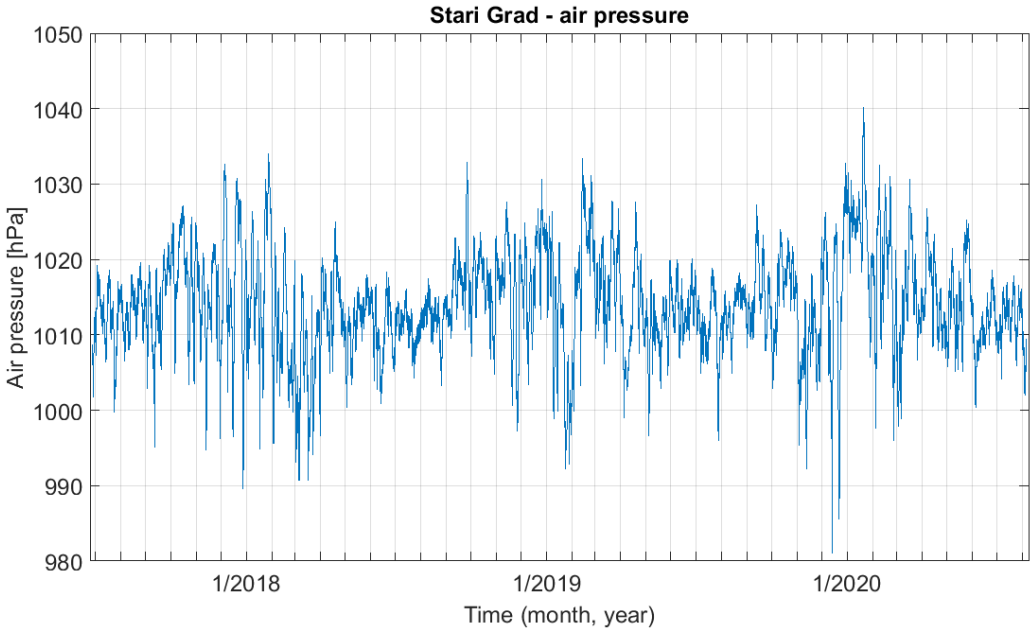

Figure 8. *Interpolated air pressure time series.*

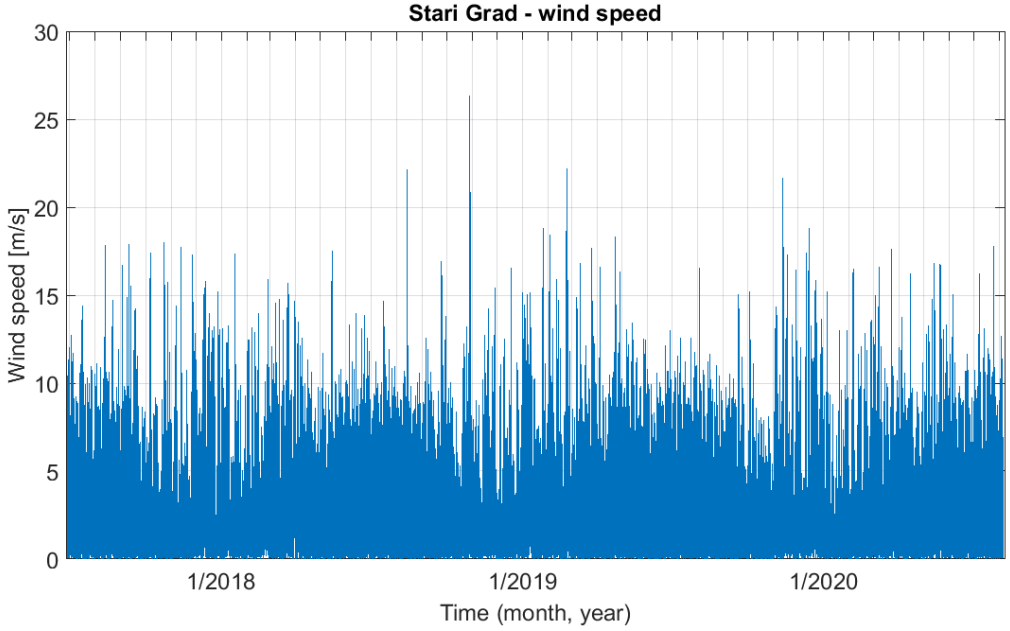

Figure 9. *Interpolated wind speed time series.*

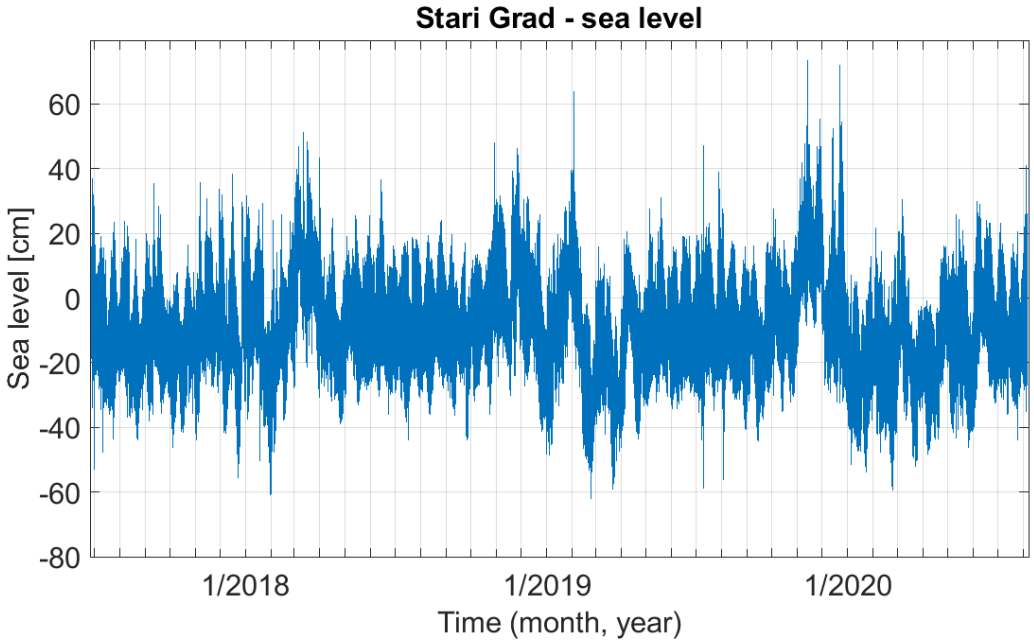

Figure 10. *Interpolated sea-level time series.*

3.2.2 Spectral analysis

As mentioned before, many processes resulting in sea-level extremes occur in Stari Grad. These processes happen at different time periods and have different amplitudes. Spectral analysis enables us to identify and distinguish between the processes. Additionally, changing the length of the window over which the spectral analysis is done can provide us with a better insight into oscillations with longer/shorter periods. For this analysis Fourier transform is applied.

Using the entire time period of the sea-level time series (3 years, 1 month and 9 days) as a window length gives a dense spectrum with distinct peaks marking oscillations at semidiurnal and diurnal tidal periods (Figure 11a). When shorter window length is choosen, e.g. 180 days, peaks with shorter periods become noticeable (Figure 11b). For even shorter window lengths, such as 30 days, these peaks are even more distinguishable (Figure 11c). If we want to examine oscillations with periods under a couple of hours, it is best to use even shorter periods, such as a day (Figure 11d). To summarize, to distinguish oscillations at periods from ~10 to 26 hours it is appropriate to use a 180 days window, for oscillations at periods from 2 to 10 hours to use a 30 day window and for oscillations at periods under two hours to use a 1 day window.

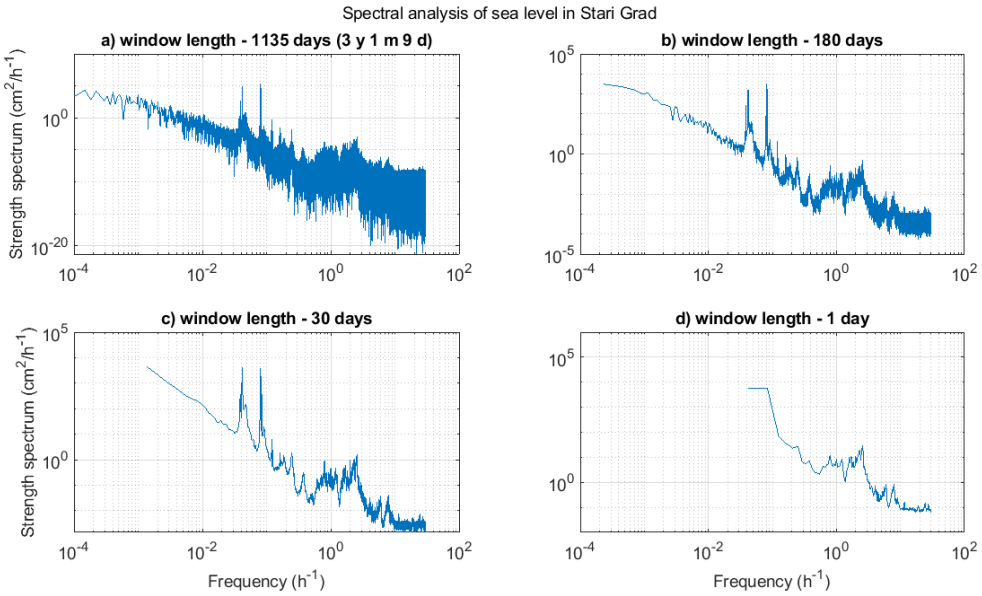

Figure 11. *Spectral analysis of sea-level time series measured in Stari Grad. Spectral analysis is done using window lengths of a) 1135 days, b) 180 days, c) 30 days and d) 1 day.*

3.2.3 Removal of tidal oscillations

Since the tidal signal in the Adriatic is well researched and known, it can be removed from the original sea-level series so the focus can be on oscillations less explored. Still, tides play an important role in sea-level changes. Sometimes low tides can mitigate severe high sea-level events. Then again, high tides can also amplify those events as seen in Figure 12. During the 13 November 2019 extreme sea-level event, maximum value of total signal was 73.56 cm, and of residual (de-tided) signal 51.17 cm.

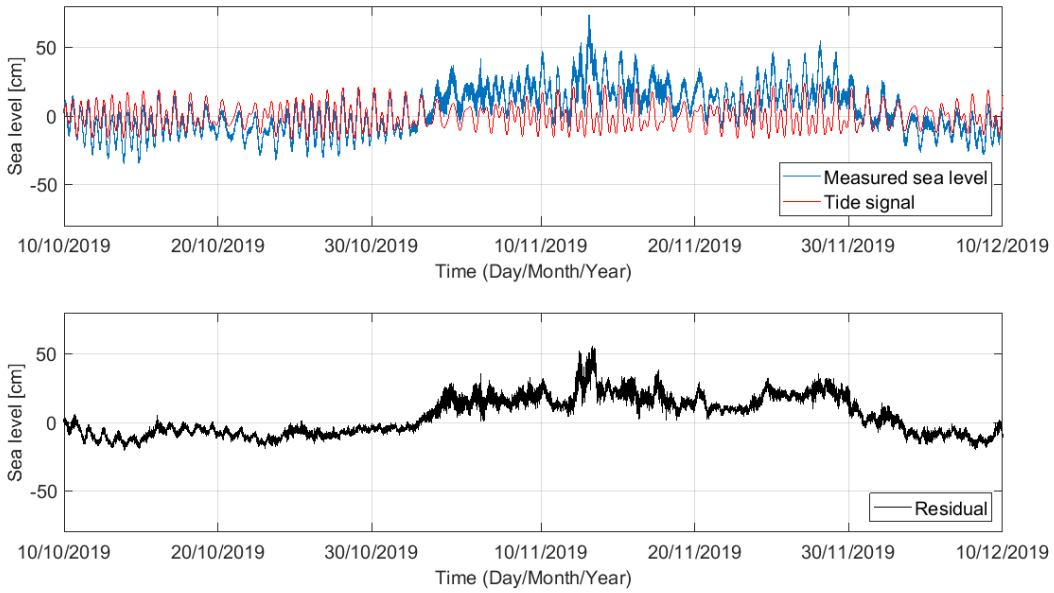

Figure 12. *(Top) measured sea level (blue), and calculated tidal signal (red); (bottom) residual signal.*

Harmonic analysis was used for estimation and removal of tidal oscillations. The MATLAB *toolbox t_tide_3* was used. [15] *Toolbox t_tide_3* as input parameters uses sea-level time series, sampling interval, start time, latitude, interference of constituents… It returns list of tidal constituents and their frequencies, phases and tidal prediction. All together, four semidiurnal (M_2, S_2, N_2, K_2) and three diurnal (K_1, O_1, P_1) harmonic constituents were estimated and removed. All further analysis are done on de-tided (residual) time series.

3.2.4 Filtering data

In order to separate the long-period sea-level extremes from the short-period sea-level extremes, I first filtered residual sea-level series using the MATLAB *kaiser* function to create filtering window of 210 min length and *filtfilt* function to filter the data. Filtered sea-level time series are shown in Figure 13, and filtered and air pressure time series in Figure 14. From now on, in the text, I refer to the low-pass (period longer than 210 min) component of filtered time series as long-period time series, and to the high-pass (periods shorter than 210 min) component as short-period time series. These two time series were studied separately further on.

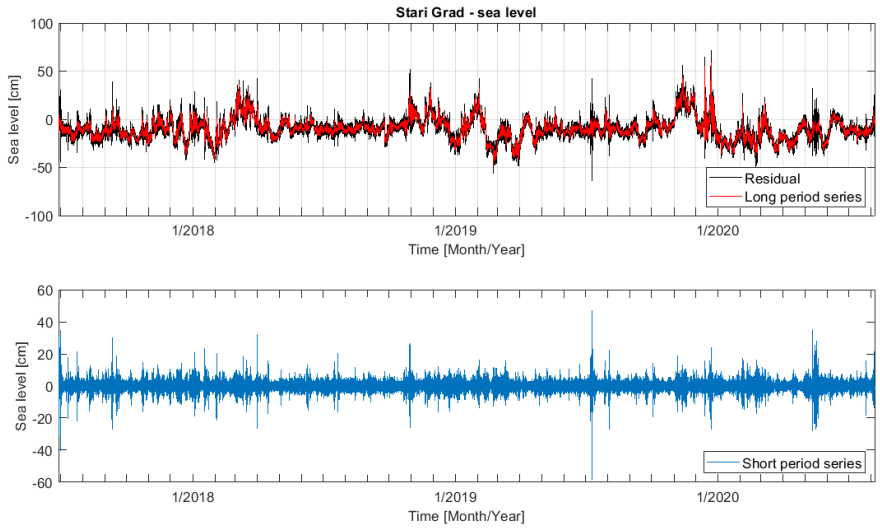

***Figure 13**. Stari Grad long-period sea-level time series (top) and short-period sea-level time series (bottom).*

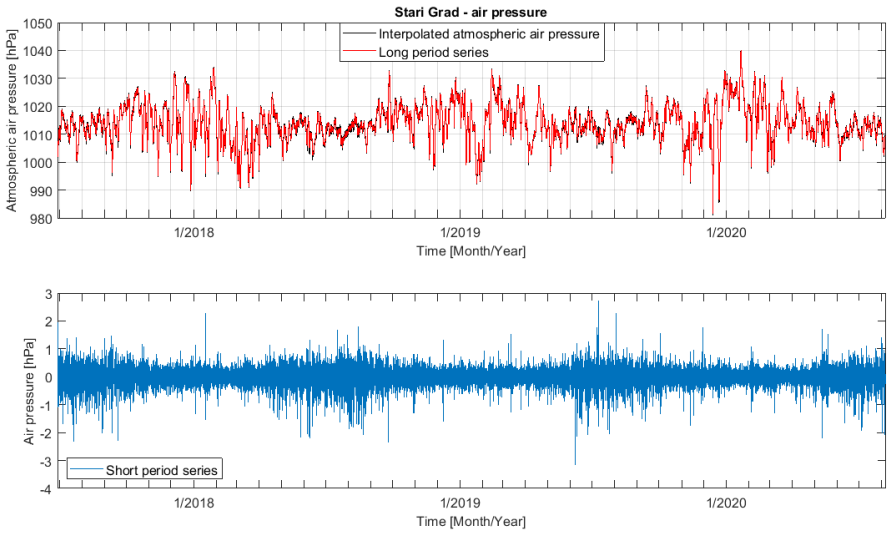

***Figure 14.** Stari Grad long-period air pressure time series (top) and short-period air pressure time series (bottom).*

3.2.5 Extraction of sea-level extremes

Positive long-period extremes were defined as those situations during which the long-period sea level surpassed the 99.7th percentile value of the corresponding time series . Negative long-period extremes were defined as those situations during which the long-period sea level was lower than the 2nd percentile of corresponding time series (Figure 15). To avoid multiplication of events during one day - as even residual sea level can oscillate above and below treshold lines due to process like the Adriatic seiche - all data above (or below for negative extremes) the percentile threshold lines measured within the 24 hour limit were classified as one event (Figure 16 and Figure 17).

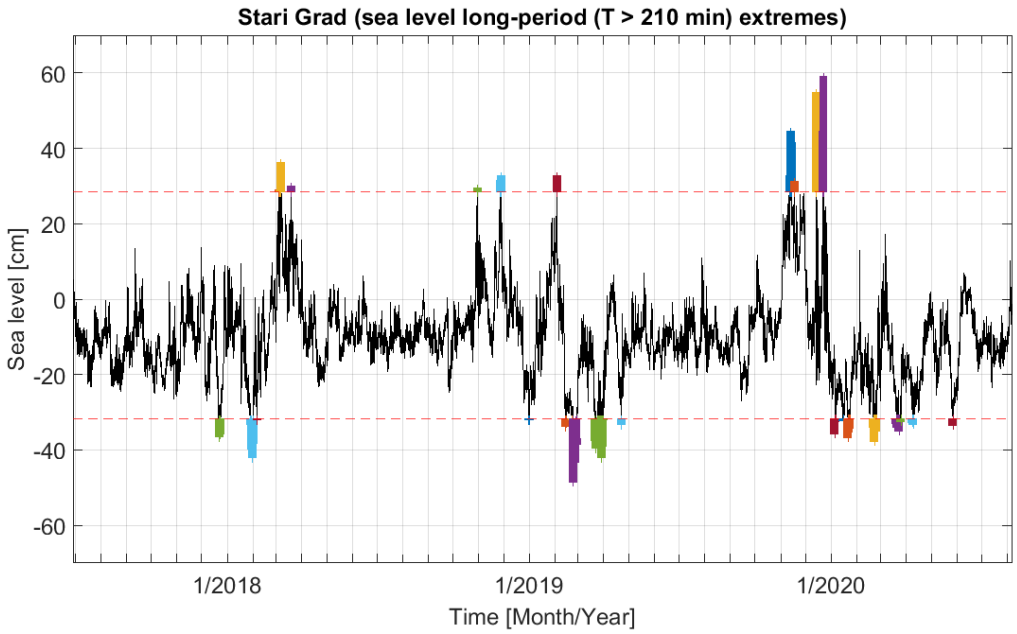

Figure 15. *Stari Grad sea-level long-period extremes (color) and long-period time series (black).*

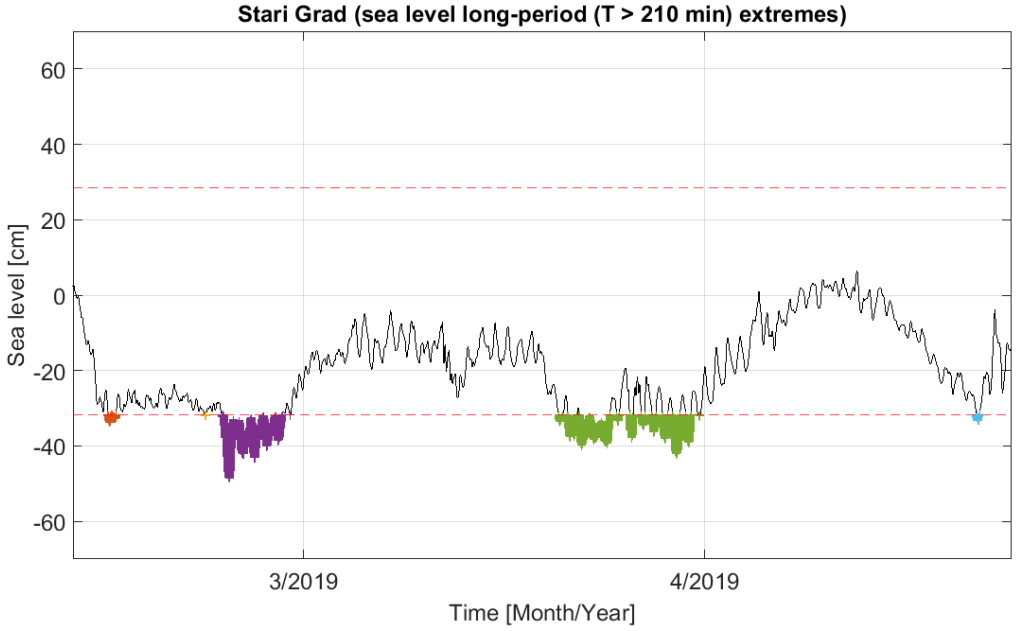

Figure 16. *A closer look into the three negative long-period extremes. Note that the extremes happening within 24 hours from each other are treated as one extreme episode (green line).*

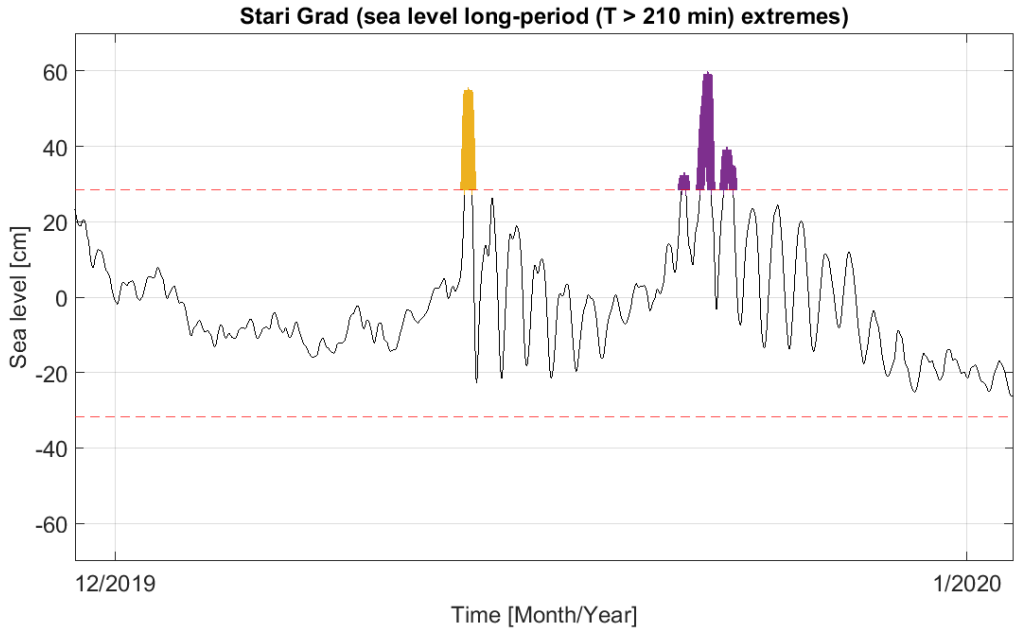

Figure 17. *A closer look into two positive long-period extremes. Note that the extremes happening within 24 hours from each other are treated as one extreme episode (purple line).*

The short-period extremes were defined as situations during which variance of short-period sea-level oscillations was higher than the 99.4 percentile value of total variance of short-period series (Figure 18). Since these oscillations fluctuate from positive to netagive on a minute time scale (periods from 2 minutes to 210 minutes), identifying the extreme episodes was not straightforward as for the long-period extremes. After identifying oscillations with variance higher than the 99.4 percentile, maximum of each episode was found. Then, an algorithm was devised which moves to the left and to the right from the maximum of the episode as long as variance of series is above the 75 percentile value (Figure 18).

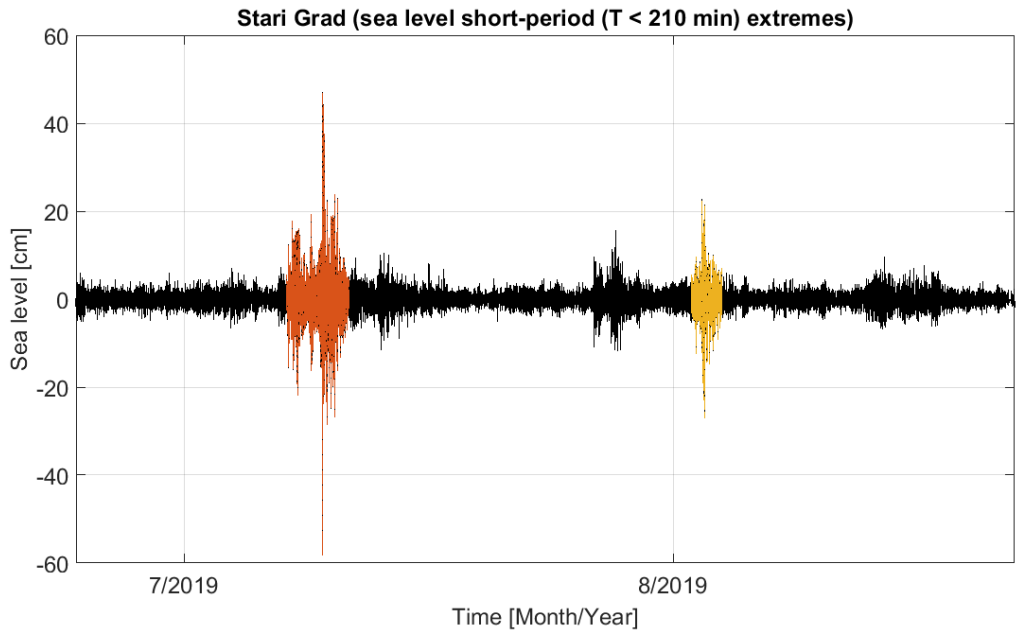

Figure 18. *A closer look at two short-period extremes.*

3.2.6 Analysis of extreme events

After identifying extreme sea-level events, I analyzed the corresponding sea-level series, and atmospheric variables: air pressure, wind speed and direction. For all extreme sea-level events, I estimated maxima (minima) of sea level, duration, and intensity (sum of all sea levels measured during duration of a episode). The atmospheric sets of data were interpolated as well. Air pressure series were also filtered using the MATLAB *kasier* and *filtfilt* functions.

3.2.7 Analysis of synoptic situations

Recognizing the local meteorological situation at Stari Grad during extreme events is necessary to understand the meteorologic forcing of the events. However, to understand the events even better, it is also essential to investigate synoptic situations which preceeded them. For this purpose, I have downloaded and analysed the mean sea level pressure field and the 10-m wind field from the ERA5 reanalysis dataset [14]; all for the dates of extreme events (at the closest available time: 00:00, 06:00, 12:00, 18:00 prior the event; as well as at the three times preceeding the event).

4 Results

4.1 Spectral analysis

Spectral analysis reveals periods at which the strongest and most consistent sea-level oscillations occur. Frequency of motion is the number of oscillations per time unit and period is the time needed for one complete oscillation - $T = \frac{1}{f}$. [16] Table 1 shows periods of the main tidal constituents in the Adriatic Sea, and their relative amplitudes (in comparison to the amplitude of the strongest M_2 tidal component).

Using the above relation, dominant periods of Stari Grad sea-level oscillations were found (Figure 19).

Table 1. *Seven main tidal constituents in the Adriatic Sea; amplitudes are given scaled with respect to the M_2 component. [8]*

Tidal constituent	Symbol	Period (hours)	Mean amplitude
Principal lunar semidiurnal	M_2	12.42	100.0
Principal solar semidiurnal	S_2	12.00	46.6
Larger lunar elliptic semidiurnal	N_2	12.66	19.2
Lunisolar semidiurnal	K_2	11.97	12.7
Lunisolar diurnal	K_1	23.93	58.4
Lunar diurnal	O_1	25.82	41.5
Solar diurnal	P_1	24.07	19.4

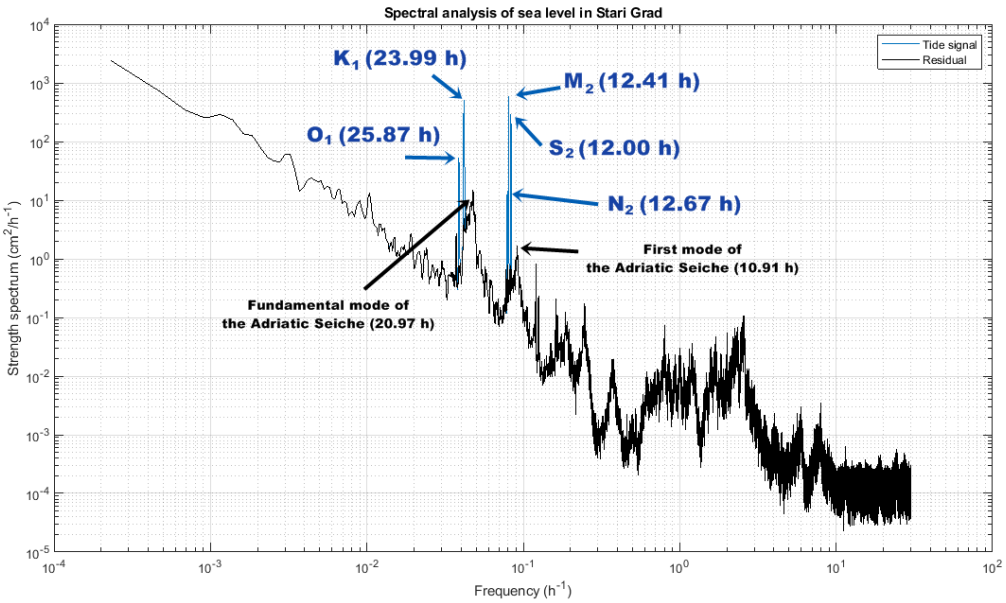

Figure 19. *Spectral analysis is applied to the Stari Grad time series of 180 days window length. Distinct peaks labeled blue represent tidal constituents, and distinct peaks labeled black represent the Adriatic seiche fundamental and first mode.*

Tides and the Adriatic seiche are basin-wide phenomena. In order to examine the higher frequency phenomena, spectral analysis is applied to time series of 24 hours window length (Figure 20). Oscillations appear within 4 distinct groups: (1) at periods from 49.8 min to 1.26 h; (2) at periods from 23.4 to 36 min; (3) at 10.2 min period; (4) at 7.8 min period. Shorter periods are most likely periods of the Stari Grad Bay local seiches. Estimated period of fundamental mode of Stari Grad bay is 10.6 min. [17] Periods of higher modes are 8.3 min and 6.1 min. [17] Oscillations at higher periods are possibly wider area seiches. [17]

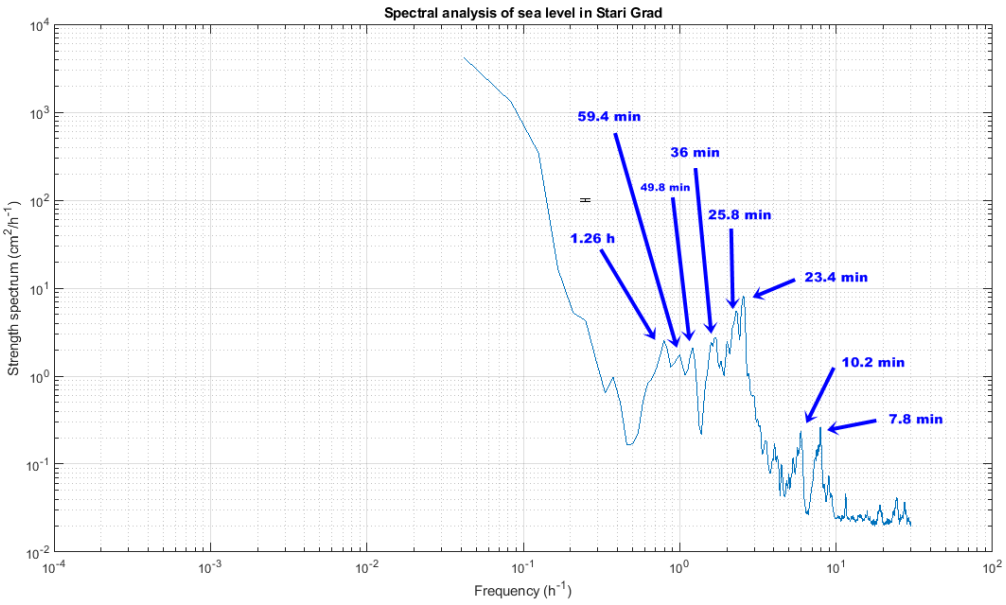

Figure 20. *Spectral analysis applied to time series of 24 hours window length: all significant peaks are given, and their periods marked.*

4.2 Extreme sea-level events

Following the methodology described in 3.2.5, I have identified 47 extreme sea-level events. Out of these 47 events, 10 events represent long-period positive extremes (Table 2), 17 events represent long-period negative extremes (Table 3) and 20 events represent short-period extremes (Table 4).

Table 2. *Chronologically sorted long-period positive sea-level extremes. Meteorologic data and synoptic situations related to all 10 episodes were further analysed.*

Long-period sea-level maxima				
Episode	Date	Max. sea-level – residual [cm]	Max. sea-level – low-pass filter [cm]	Duration
1	03.03.2018.	27.4038	28.9011	1h 24min
2	06.03.2018.	35.2677	36.2591	1d 5h 34min
3	18.03.2018.	31.2651	29.9174	2h
4	29.10.2018.	40.9263	29.4270	1h 12min
5	27.11.2018.	37.0830	32.7993	5h 12min
6	03.02.2019.	35.2462	32.6836	3h 57min
7	13.11.2019.	44.1509	44.6542	1d 6h 9min
8	17.11.2019.	33.2737	31.2251	2h 50min
9	13.12.2019.	53.2870	54.6993	6h 29min
10	22.12.2019.	65.3004	59.0738	1d 21h

Table 3. *Chronologically sorted long-period negative sea-level extremes. Meteorologic data and synoptic situations related to the 10 strongest (shaded) episodes were further analysed.*

Long-period minima				
Episode	Date	Min. sea-level – residual [cm]	Min. sea-level – low-pass filter [cm]	Duration
1	22.12.2017.	-35.8313	-36.4394	1d 20h 6min
2	30.01.2018.	-40.7519	-41.9463	3d 13h 40min
3	05.02.2018.	-34.5157	-32.0605	2h 14min
4	31.12.2018.	-32.1857	-32.0419	1h 30min
5	14.02.2019.	-34.0898	-33.7138	15h 1min
6	21.02.2019.	-32.4851	-31.8982	2h 18min
7	23.02.2019.	-49.2242	-48.6238	5d 7h 48min
8	29.03.2019.	-40.7800	-42.1075	10d 22h 11min
9	22.04.2019.	-33.5793	-33.3653	5h 15min
10	05.01.2020.	-38.8383	-35.6288	21h 36min
11	16.01.2020.	-30.8328	-32.2692	3h
12	21.01.2020.	-36.7362	-36.7797	2d 7h 16min
13	22.02.2020.	-41.0570	-37.8805	2d 22h 40min
14	23.03.2020.	-30.5993	-35.0460	3d 22h 9min
15	25.03.2020.	-31.7539	-32.3786	3h 23min
16	09.04.2020.	-33.4443	-33.3331	1d 2h 36min
17	27.05.2020.	-33.0267	-33.4319	6h 13min

Table 4. *Chronologically sorted short-period sea-level extremes. Meteorologic data and synoptic situations related to the 10 strongest (shaded) episodes were further analysed.*

Short-period extremes			
Episode	Date	Max. wave height [cm]	Duration
1	28.06.2017.	41.24	6h 12min
2	28.06.2017.	33.96	1d 5h 30min
3	01.07.2017.	49.95	1d 21h 37min
4	12.07.2017.	27.15	1d 7h 2min
5	24.07.2017.	43.02	1d 6h 46min
6	11.09.2017.	46.02	2d 16h 47min
7	17.09.2017.	34.49	2d 5h 24h
8	03.01.2018.	31.84	2d 11h 48min
9	17.01.2018	38.61	1d 18h 3min
10	03.02.2018.	40.51	1d 12h 24min
11	17.03.2018.	32.41	1d 20h 54min
12	31.03.2018.	58.81	1d 17h 8min
13	21.07.2018.	36.81	18h 12min

14	29.10.2018.	50.84	3d 20h 47min
15	09.07.2019.	104.95	3d 22h 50min
16	02.08.2019.	34.86	1d 23h 13min
17	22.12.2019.	33.51	4d 6h 38min
18	11.05.2020.	62.89	1d 14h 5min
19	17.05.2020.	44.75	7d 5h 6min
20	24.07.2020.	25.59	23h 45min

Monthly distributions of long-period maxima episodes of are given in the first column of Figure 21. Long-period maxima episodes usually occur during late autumn/early winter and late winter/early spring. They last slightly more during late autumn/early winter, when they are also most intense.

Monthly distributions of long-period minima episodes are given in the second column of Figure 21. Long-period minima episodes dominantly appear during winter and spring months with an occurrence peak in February. However, the episodes are longest and most intense during March. The long-period minima episodes also occasional occur during autumn and early spring.

Monthly distributions of short-period extremes are given in the third column of Figure 21. The short-period extremes occur throughout the year. Still, they are most frequent during July (6 episodes), and they are strongest in May and July. Additionally, the longest duration of short-period extremes occur in May.

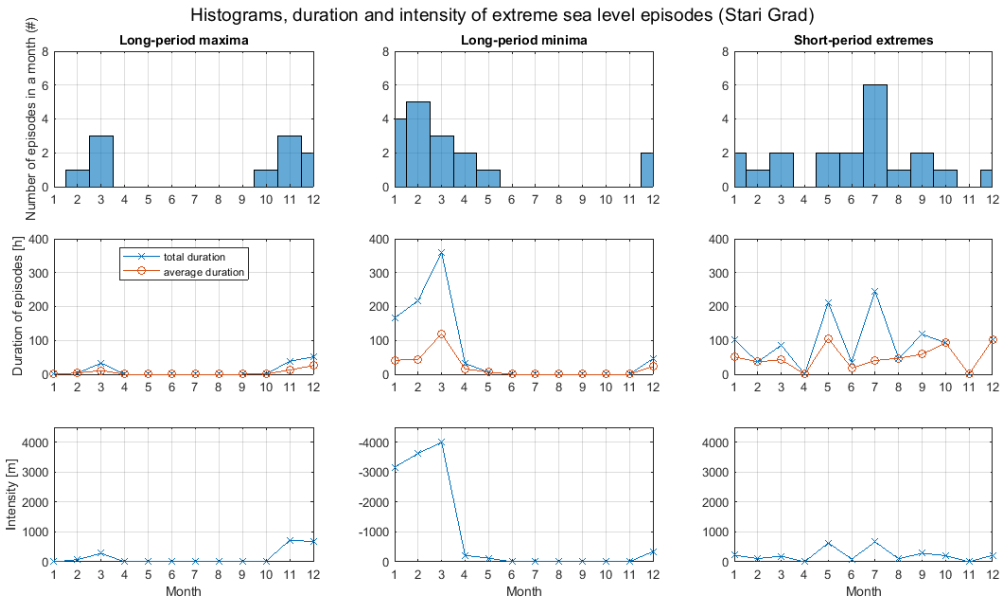

***Figure 21**. Number of events per month (top), duration per month (middle) and intensity per month (bottom) of extreme sea-level episodes in Stari Grad.*

4.3 Air pressure and wind during extreme sea levels

4.3.1 Positive long-period extremes

Air pressure and wind measured at the Stari Grad tide gauge location were analyzed for the 10 selected episodes of positive long-period extremes. I have noticed two similar types of weather situations related to the these extremes.

The first situation is characterised by a presence of lower than average air pressure (< 1010 hPa) during a couple of days surrounding the event, and strong SE winds blowing before the episode. An example is given in Figures 22 and 23 in which meteorological measurements done during the episode of 29th of October, 2018 are depicted. One can clearly see that during the episode air pressure was lower than usual for 1 standard deviation. As for the wind speeds, these were up to ~10 m/s during the episode, but up to 20 m/s before the episode. The strongest winds were blowing from the ESE (Figure 23).

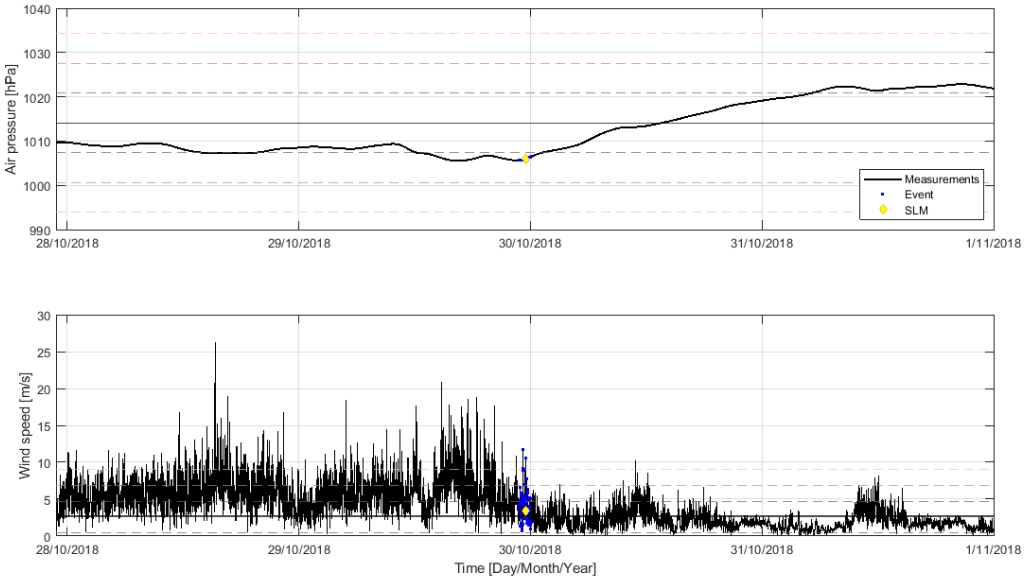

Figure 22. *Positive long-period episode of 29th of October, 2018. Air pressure time series (top) and wind speed time series (bottom). SLM in the legend stands for the sea-level maximum. In both plots, the solid black line shows three year mean value, and dashed reddish lines show 1, 2 and 3 standard deviations.*

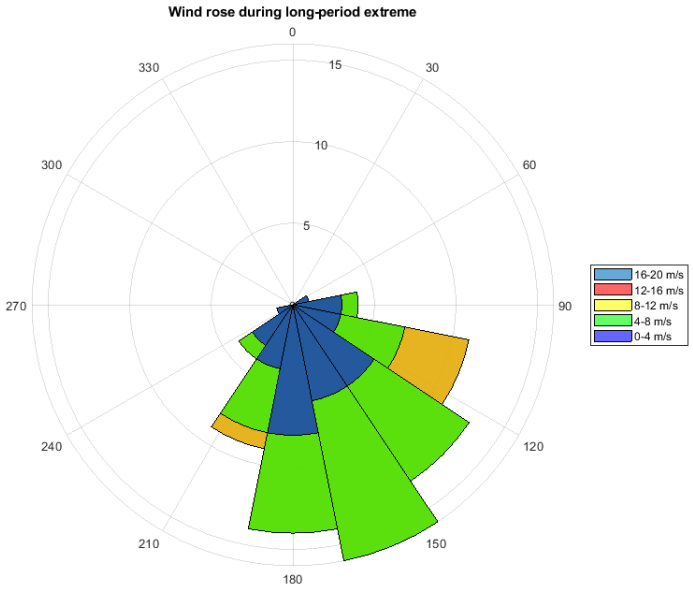

Figure 23. *Wind rose for the episode of 29th of October, 2018.*

The second type of situation corresponds to an extremely low air pressure (< 990 hPa) for a couple of days during the event, and winds of very high speeds precisely during the episode, not before or after. An example is given in Figures 24 and 25 in which meteorological measurements done during the episode of 13th of December, 2019 are depicted. During the episode air pressure was lower than its mean value by much more than 3 standard deviations. The wind speed reached up to 18 m/s with the strongest winds blowing from the SE, and some moderate NW winds (Figure 25).

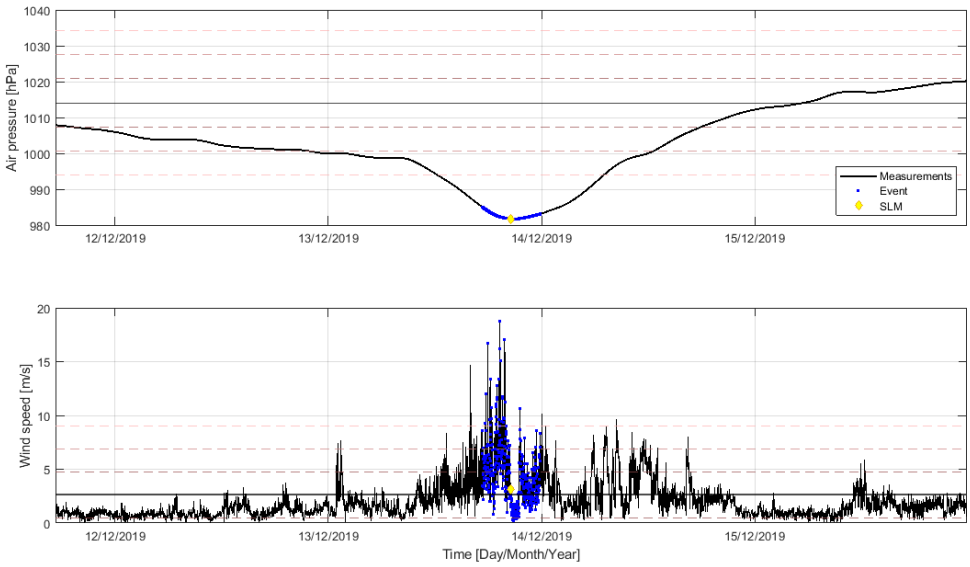

Figure 24. *Positive long-period episode on 13th of December, 2019. Air pressure time series (top) and wind speed time series (bottom). SLM in the legend stands for the sea-level maximum.*

In both plots, the solid black line shows three year mean value, and dashed reddish lines show 1, 2 and 3 standard deviations.

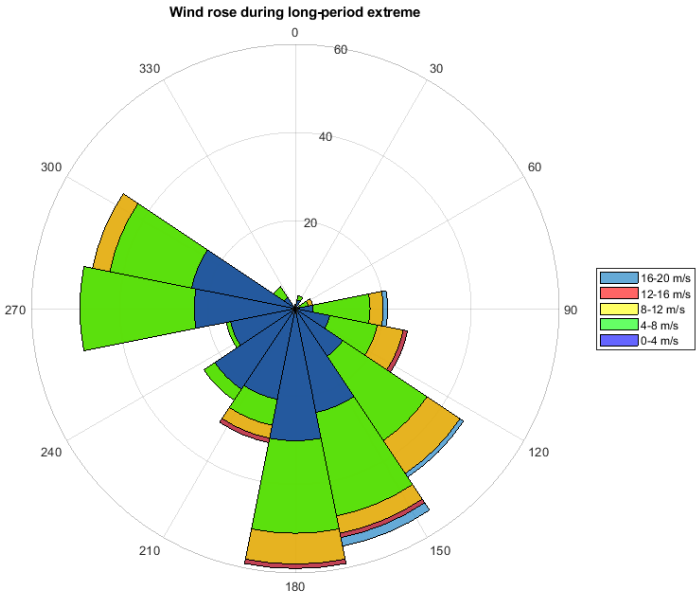

Figure 25. *Wind rose for the episode of 13th of December, 2019.*

4.3.2 Negative long-period extremes

Negative long-period extremes can also be associated to two types of situations, both of which are characterised by very high atmospheric pressure (> 1020 hPa). Additionally, the first situation is associated with strong NE (i.e. *bora*) winds, and the second to relatively calm situations during which light SE winds interchange with moderate NW wind.

First situation is depicted in Figures 26 and 27 in which meteorological measurements done during the episode of 5th of January, 2020 are given. During the episode air pressure was higher than average by more than 2 standard deviations. Before and after the episode air pressure was also higher than usual, but not as high as during the episode. Strong wind with speed up to 15 m/s was blowing just before the episode. During the episode wind was moderate with a NE direction.

The second characteristic situation is depicted in Figures 28 and 29 in which meteorological measurements done during the episode of 23rd of January, 2020 are given. Right before and during the beginning of the episode, air pressure was extremely high – higher than average by more than 3 standard deviations. During the rest of the episode, air pressure was dropping, but was still higher than usual. Day and a half before the episode strong wind was blowing. However, during the episode SE wind was relatively light, with a moderate NW peak.

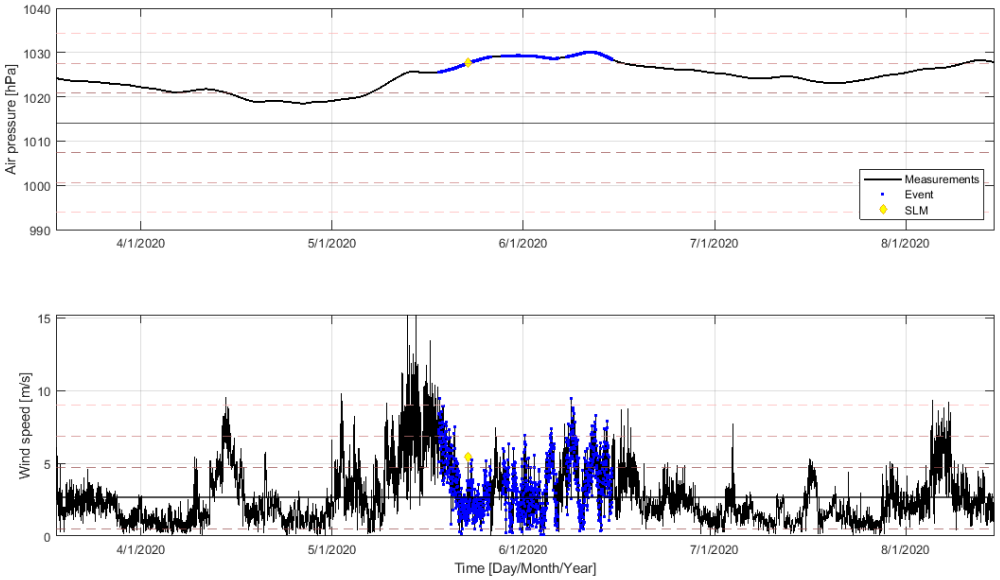

Figure 26. *Negative long-period episode on 5th of January, 2020. Air pressure time series (top) and wind speed time series (bottom). SLM in the legend stands for sea-level minimum.*

In both plots, the solid black line shows three year mean value, and dashed reddish lines show 1, 2 and 3 standard deviations.

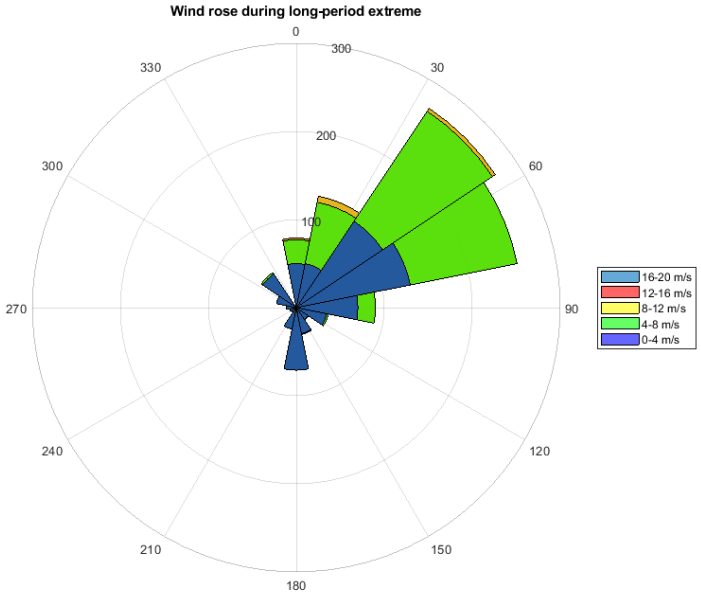

Figure 27. *Wind rose for the episode of 5th of January, 2020.*

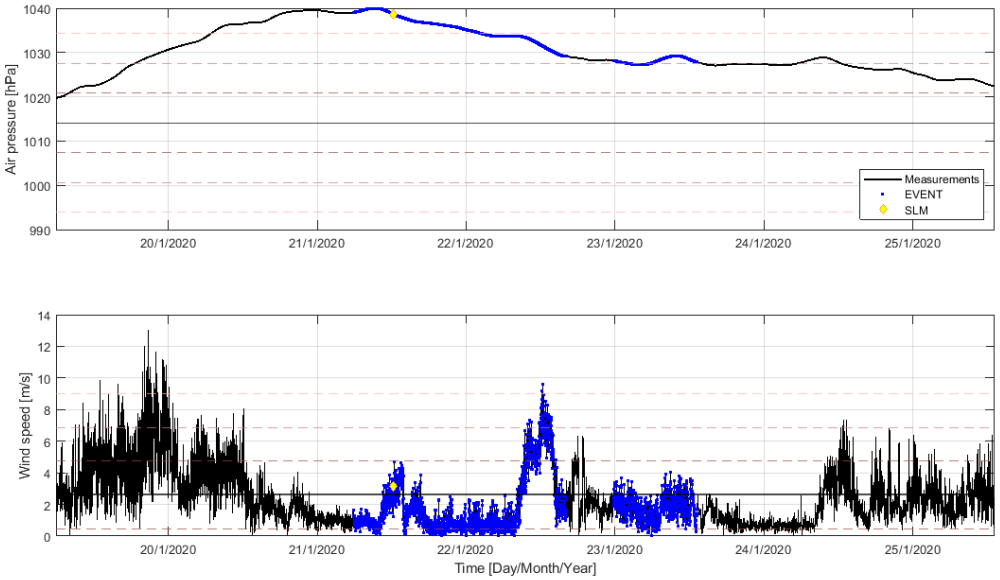

Figure 28. *Negative long-period episode on 21st of January, 2020. Air pressure time series (top) and wind speed time series (bottom). SLM in the legend stands for the sea-level minimum.*

In both plots, the solid black line shows three year mean value, and dashed reddish lines show 1, 2 and 3 standard deviations.

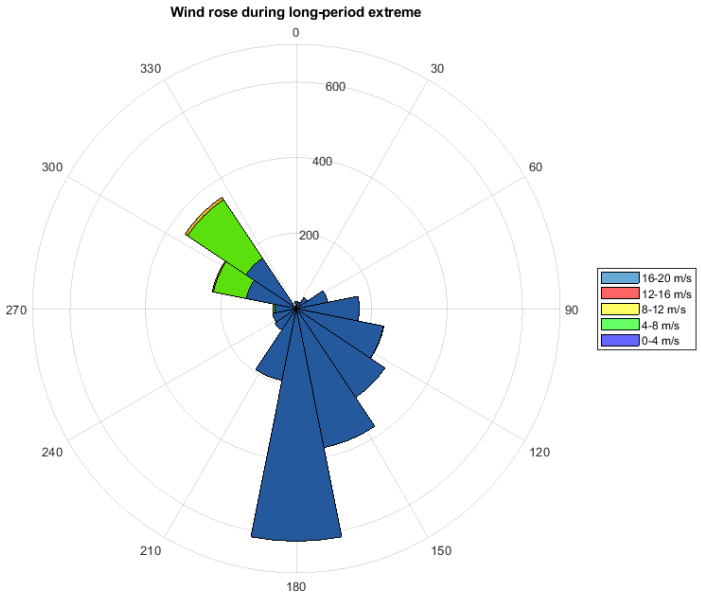

Figure 29*. Wind rose for the episode of 21st of January, 2020.*

4.3.3 Short-period extremes

All of short-period extreme sea oscillations episodes had one common characteristic – sudden pronounced changes of short-period air pressure component . As for the unfiltered air pressure, it was either lower than average or normal during all episodes. Situations characterised with lower than average air pressure are usually also associated with strong SE winds (Figure 30 and Figure 31), and situations characterised with normal pressure are usually associated with moderate winds of no dominant direction or with no winds at all (Figure 32 and Figure 33).

The first situation is depicted in Figures 30 and 31 in which meteorological measurements done during the episode of 31st of March, 2019 are given. Air pressure during the episode was lower than average by more than 2 standard deviations. Before and after the episode air pressure had almost the same values as the mean value. Short-period component of air pressure reveals pronounced oscillations during the entire episode. The strongest oscillation with wave amplitude of almost 1.5 hPa happened right after the sea-level extreme and lasted for 14 minutes. The SE and E winds were blowing before and during most of the episode. Towards the end of the episode wind speed decreased and was around 3 m/s.

The second situation is shown in Figures 32 and 33 in which meteorological measurements done during the episode of 7th of July, 2019 are given. During the entire episode, air pressure was either slightly lower than average or average (almost equal to its mean value). On the other hand, short-period component of air pressure reveals four sudden oscillation during the episode. The strongest one, with the wave amplitude of 4.5 hPa and almost one hour duration, happened right after the sea-level extreme. It can also be noticed that most of these sudden changes correspond to sudden pronounced changes of wind speed. Winds were light during most of the episode, except during the times of pronounced air pressure oscillations. During the last part of the episode there were no more short-period air pressure changes and wind speed was moderate with no preferred direction.

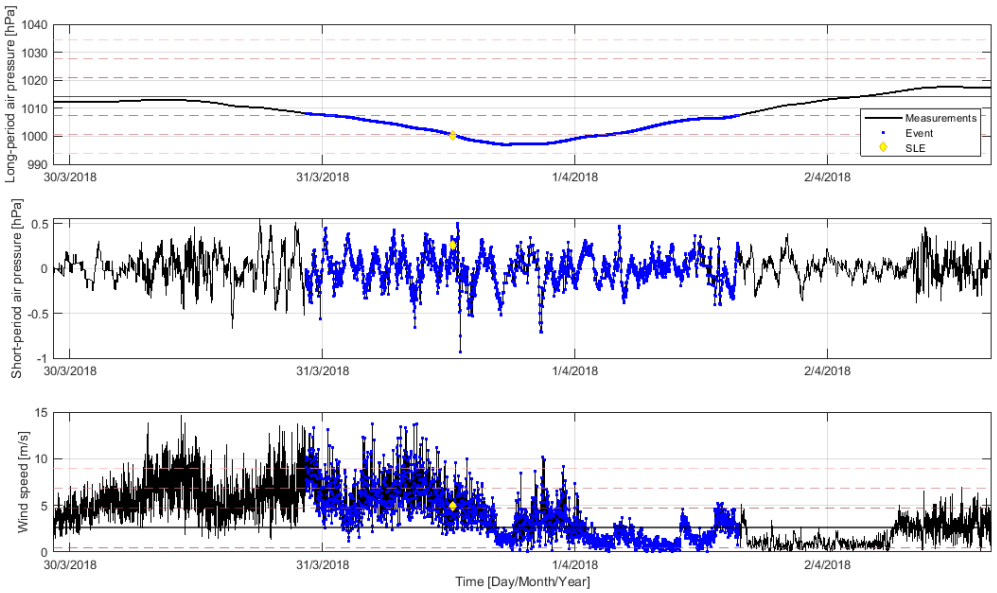

Figure 30. *Short-period episode on 31st of March, 2018. Long-period air pressure time series (top), short-period air pressure time series (middle) and wind speed time series (bottom). SLE in the legend stands for the sea-level extreme.*

In all plots, the solid black line shows three year mean value, and dashed reddish lines show 1, 2 and 3 standard deviations.

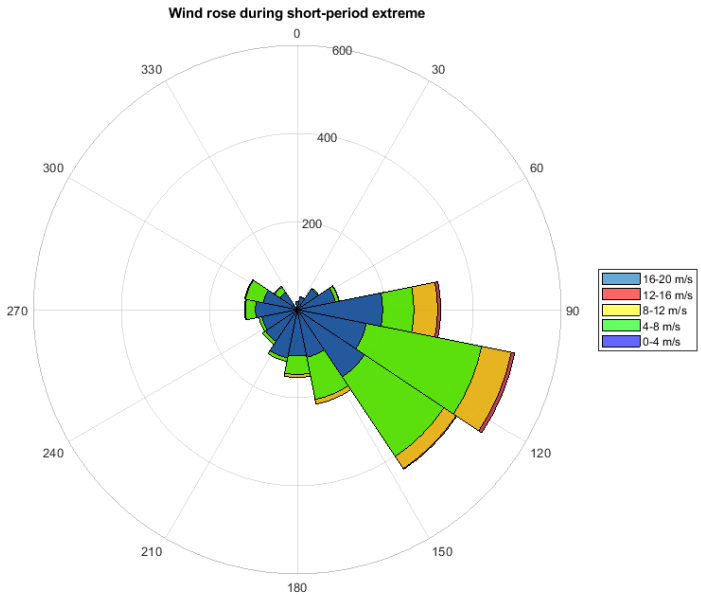

Figure 31. *Wind rose for the episode of 31st of March, 2018.*

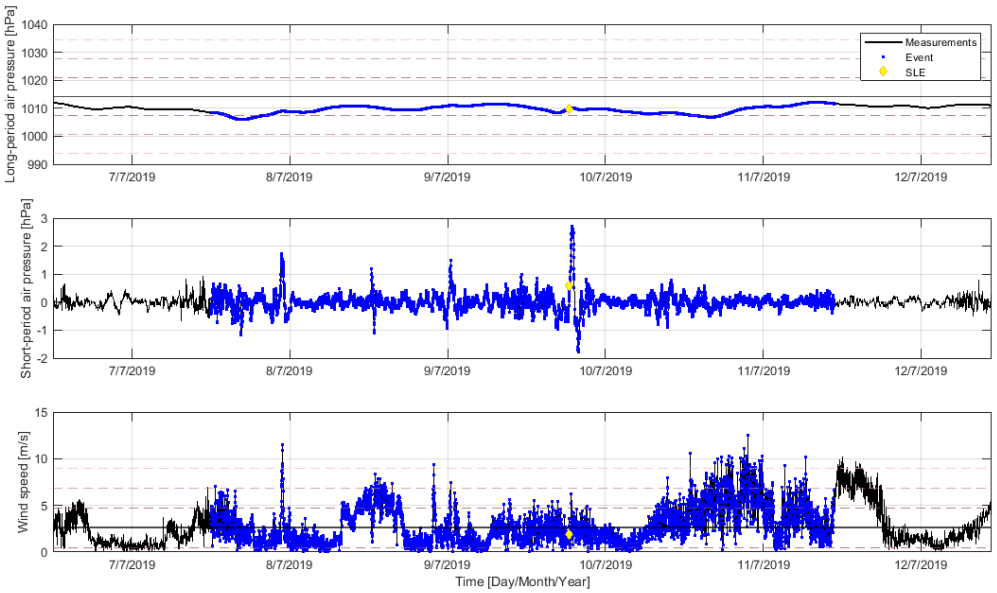

***Figure 32**. Short-period episode on 7th of July, 2019. Long-period air pressure time series (top), short-period air pressure time series (middle) and wind speed time series (bottom).*

In all plots, the solid black line shows three year mean value, and dashed reddish lines show 1, 2 and 3 standard deviations.

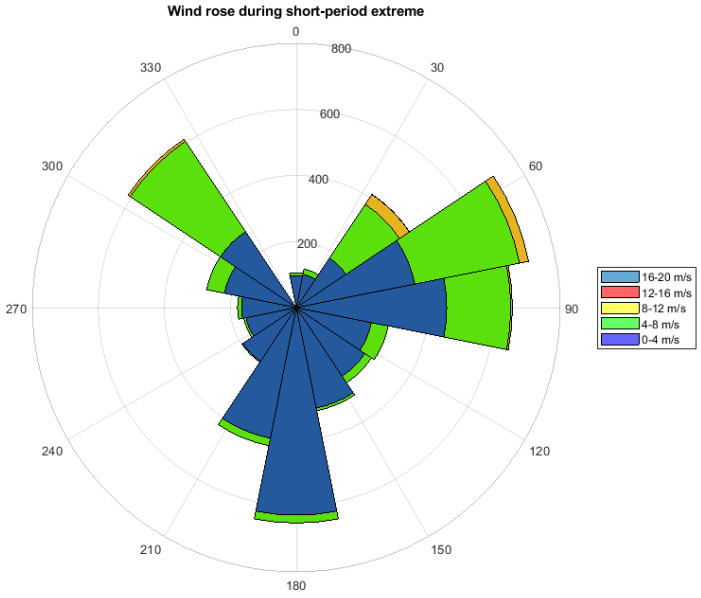

***Figure 33.** Wind rose for the episode of 7th of July, 2019.*

4.4 Synoptic situations analysis

Using the ERA5 reanalysis data, synoptic situations related to all episodes of extreme sea levels were additionally analyzed. Two types of synoptic situations for every category of extreme events were recognized.

4.4.1 Positive long-period extremes

Positive long-period sea-level extremes appear during presence of low pressure system (cyclone) over the Gulf of Genoa, or over the Adriatic. In both cases a strong SE wind blows over the Adriatic Sea. Example of the first situation is given in Figure 34 for the episode of 29th of October, 2018 and for the second situation in Figure 35 for the episode of 13th of December, 2019.

During the episode of 29th of October, low pressure field was first found over the Genoa Bay with minimum pressure values of 998 hPa. Over the next 18 hours, the center of the cyclone propagated towards the north reaching the Western Alps with minimum pressure values dropping to 982 hPa. Northward propagation of the cyclone resulted in intensification of the pressure gradients over the Adriatic Sea and strengthening of the SE wind.

At the beginning of the episode of 13th of December, air pressure over the Adriatic area was slightly lower than average (1002 hPa). However, presence of extremely low pressure area was detected over the northwestern Europe (974 hPa). During the next 12 hours the low pressure area propagated towards the southeast. At the same time another cyclone formed over the Western Alps with the minimum pressure values of 986 hPa, and related pressure gradients caused SE wind to blow over the Adriatic area. During the next six hours this cyclone propagated towards the northern Adriatic causing strong southeast to south winds over the Adriatic.

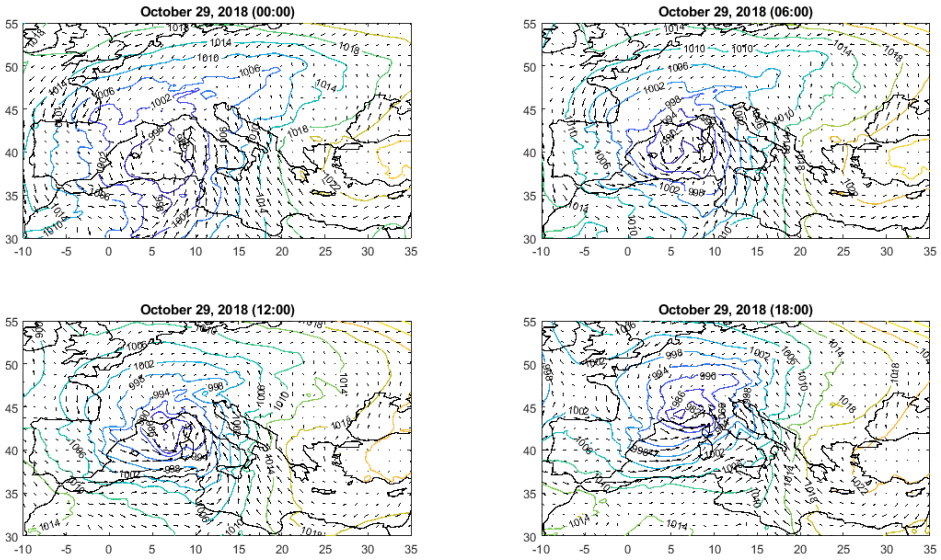

Figure 34. *The mean sea-level pressure field and 10-m wind vectors over the Mediterranean on 29th of October, 2018.*

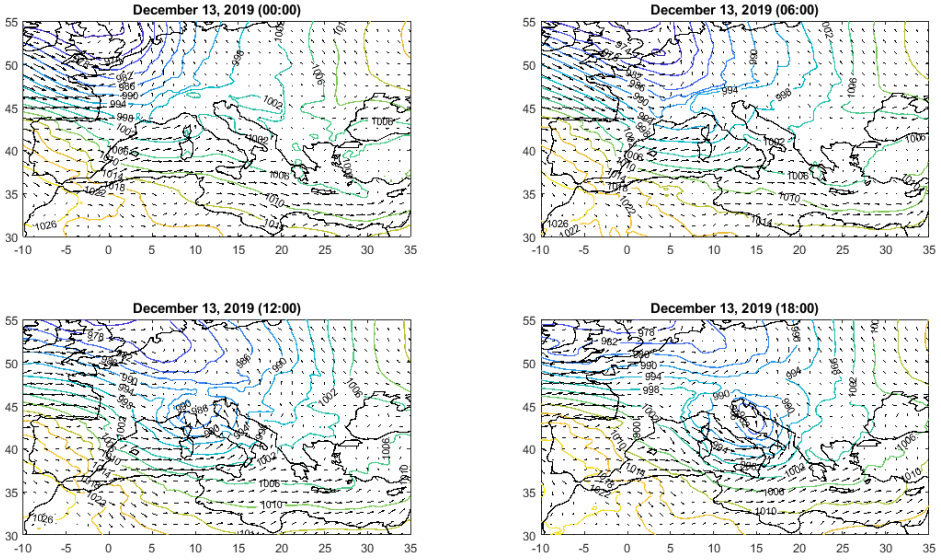

Figure 35. *The mean sea-level pressure field and 10-m wind vectors over the Mediterranean on 13th of December, 2019.*

4.4.2 Negative long-period extremes

Negative long-period extremes are associated with the high atmospheric pressure field over the area which is further associated with either strong NE winds (Figure 36; the episode of 5th of January, 2020), or no winds at all (Figure 37; the episode of 21st of January, 2020).

Right before the episode of 5th of January, 2020, air pressure over the western Europe was extremely high (maximum value of 1038 hPa), and air pressure over the eastern Europe was average (~1014 hPa). This pressure gradient caused NW winds over the Adriatic. Over the next

18 hours the higher air pressure area propagated towards the east, and the lower air pressure area towards the west. Wind direction over the Adriatic shifted accordingly – from NW to N to NE. During the episode there was a small cyclone over the Aegean Sea (minimal value of 1006 hPa). The observed pressure gradients over the Adriatic caused the strongest NE winds precisely during the episode.

Synoptic situation of the episode of 21st of January, 2020 was somewhat static. Before and during the episode air pressure over the central Europe was extremely high (maximum value of 1046 hPa) and relatively normal over the southwest Mediterranean. Situation stayed relatively the same for the next 18 hours. During the episode, air pressure over the Adriatic was extremely high with no winds at all.

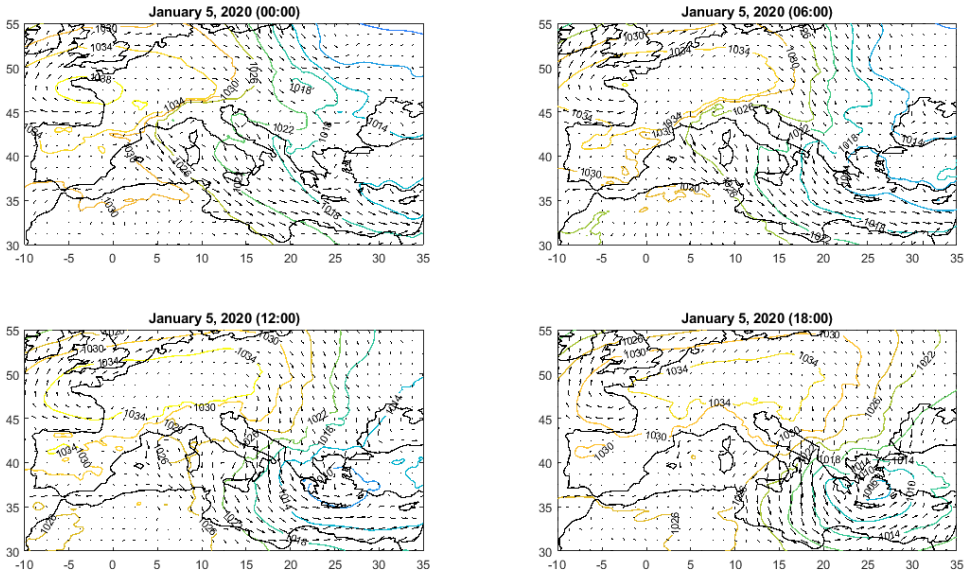

Figure 36. *The mean sea-level pressure field and 10-m wind vectors over the Mediterranean on 5th of January, 2020.*

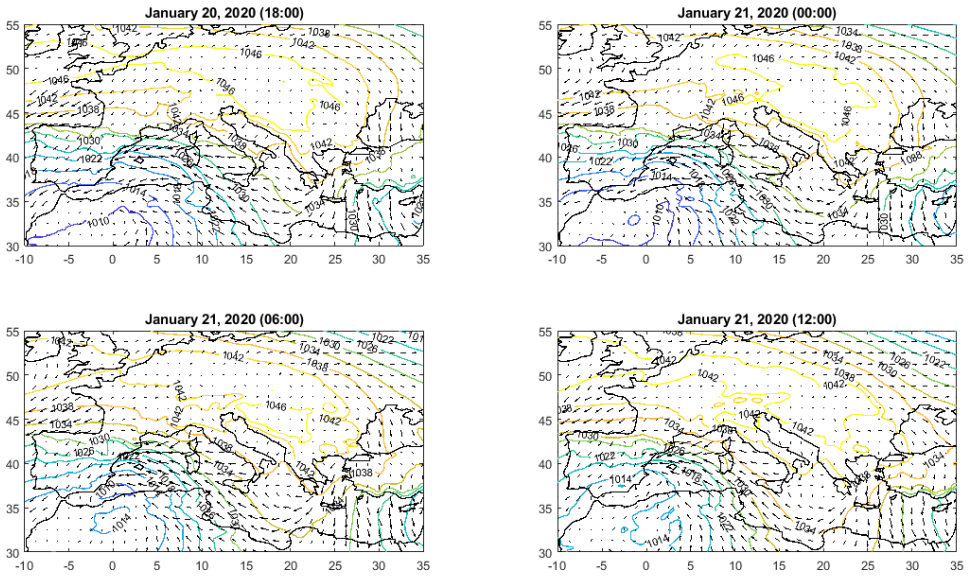

Figure 37. *The mean sea-level pressure field and 10-m wind vectors over the Mediterranean on 21st of January, 2020.*

4.4.3 Short-period extremes

Short-period sea level extremes are noticed during the two types of atmospheric situations corresponding to both "bad" (low pressure, strong SE wind) weather (Figure 38; the episode of 31st of March, 2018), and "nice" (normal/high pressure, no wind) weather (Figure 39, the episode of 9th of July, 2019).

Before the episode of 31st of March, 2018, air pressure over the western Europe was lower than average (minimal value of 994 hPa). Over the eastern part of the Mediterranean air pressure was slightly higher than average, causing strong pressure gradient over the Adriatic, where air pressure was initially average (~1010 hPa). Over the next 18 hours area of low air pressure propagated to the east (during the episode air pressure above the Adriatic was ~998 hPa). Strong SE and S winds were blowing during the whole episode.

The episode of 9th of July, 2019 is an example of relatively calm synoptic situation over the Mediterranean. There were no areas of extreme air pressure and no pressure gradients, meaning there were no winds blowing over the Adriatic. Air pressure over the Adriatic was fairly average (~1012 hPa).

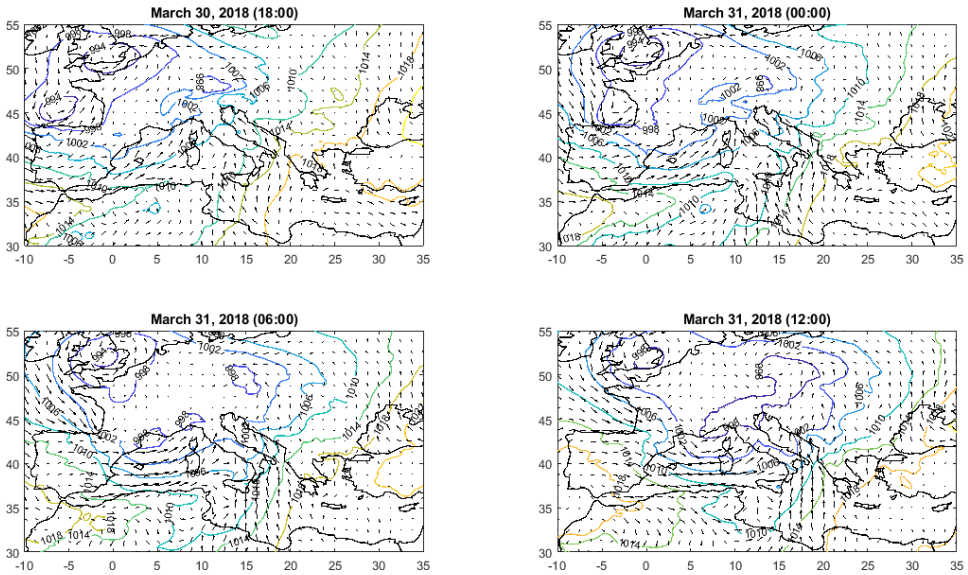

Figure 38. *The mean sea-level pressure field and 10-m wind vectors over the Mediterranean on 31st of March, 2018.*

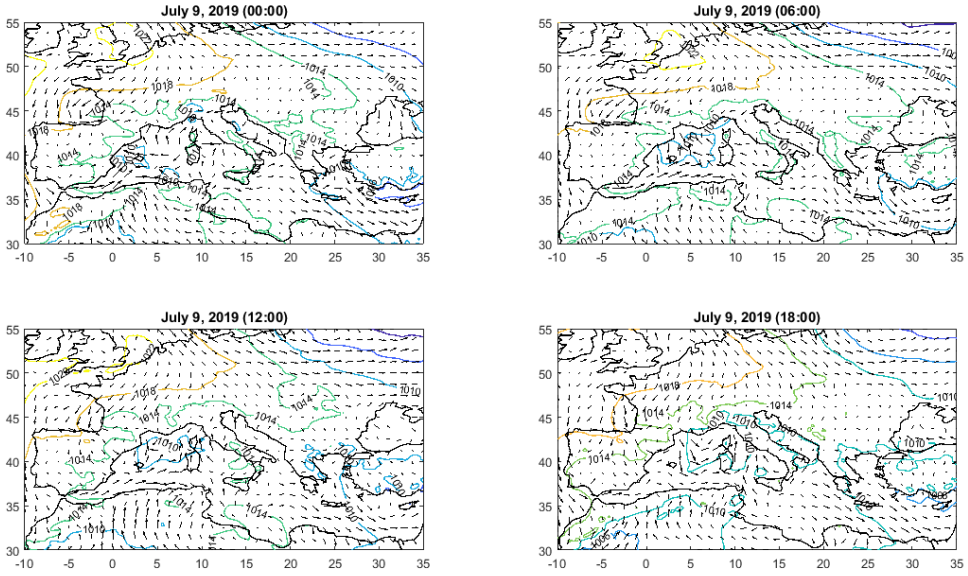

Figure 39*. The mean sea-level pressure field and 10-m wind vectors over the Mediterranean on 9th of July, 2019.*

5 Conclusion

Analysis of three years measurements reveal that numerous sea-level extremes (some of which are exceptionally strong) occur in Stari Grad. It is of particular importance that the short-period extremes, of which the strongest ones are meteotsunamis, are occasionally coincident with positive long-period extremes contributing with up to 50 percent to total sea level height – thus implying existence of a double danger phenomena - meteotsunami + storm surge (eg. episode of 29th of October, 2018).

Low air pressure causes increase in sea level (the inverse barometer effect) – a decrease in air pressure of 1 hPa corresponds to an increase in sea level of 1 cm. [18] Additionally, S/SE wind blowing over the Adriatic pushes water mass towards the closed end of the basin, increasing sea level especially in the northern parts of the Adriatic, and somewhat less in the central Adriatic. [6] On the other hand, high air pressure causes decrease in sea level (also through the inverse barometer effect) and NE wind (*bura*) pushes water mass away from the Croatian coast. [1] Regarding short-period sea-level oscillations, when air pressure disturbances propagate over the open sea, they generate long ocean waves. If the speed of air pressure disturbances is the same as the speed of long ocean waves, Proudman resonance will occur. Sea-level oscillations can then be intensified up to 10 times when compared to the inverse barometer effect. Long ocean waves can also be amplified near the coast due to narrowing in bays, harbour resonance, etc. (Stari Grad and Vela Luka bay). [1]

Analyses of meteorological measurements and synoptic situations (ERA5 reanalysis) can be compared. Meteorological measurements for positive long-period extremes of 29th of October, 2018 and 13th of December, 2019 show lower than usual air pressure over Stari Grad. Also, wind rose shows SE wind direction for both episodes. Analysis of the synoptic situation over the Mediterranean also reveals lower air pressure with strong SE winds over the central Adriatic. Data also matches for negative long-period extremes where both measurements and the ERA5 analysis show high air pressure over the area of Stari Grad with NE winds for the first episode, and no winds for the second. The same can be said for the short-period extremes, where meteorological measurements also match reanalysis of synoptic situation. However, the most important feature of the short-period extremes are pronounced short-period air pressure oscillations. These are of such a small spatial and temporal extent that are non-reproducible with global (and even regional) models, such as the ERA5 model. Thus, to explore the short-period sea level extremes, meteorological measurements at the endangered location are necessary.

Even though three years of measurements provided much needed materials for this research, longer measurements would give an even better insight into the sea-level extremes, and allow for a more detailed statistical analysis including the estimation of return periods. More extremes would be extracted and analysed, and more accurate monthly distributions could be obtained.

This would be especially important for the short-period extremes since they seemingly occur throughout the year.

Nevertheless, this research shows that Stari Grad is a flood-prone area, and it confirms the well known fact that the Adriatic Sea is a storm surge and a meteotsunami *hotspot*. [1] Many other sea-level phenomena leading to floods can be observed in the Adriatic Sea, making it one of the greatest nature's research labs in the world.

6 References

[1] Vilibić I., Šepić J., Pasarić M., Orlić M., *The Adriatic Sea: A Long-Standing Laboratory for Sea Level Studies*, Pure and Applied Geophysics, **174**, 3765-3811 (2017)

[2] Sheppard, C., *World Seas: An Environmental Evaluation*, Academic Press, 2018

[3] Šepić, J., Međugorac, I., Janeković, I., Dunić, N., Vilibić, I., *Multi-Meteotsunami Event in the Adriatic Sea Generated by Atmospheric Disturbances of 25–26 June 2014.*, Pure and Applied Geophysics. ***173***, 4117–4138, doi*: 10.1007/s00024-016-1249-4.* (2016)

[4] Antonioli, F., Anzidei, M., Lambeck, K., Auriemma, R., Gaddi, D., Furlani, S. et al., *Sea-level change during the Holocene in Sardinia and in the northeastern Adriatic (central Mediterranean Sea) from archaeological and geomorphological data*, Quaternary Science Reviews, **26**, 2463–2486 (2007)

[5] Church, J.A., P.U. Clark, A. Cazenave, J.M. Gregory, S. Jevrejeva, A. Levermann, M.A. Merrifield, G.A. Milne, R.S. Nerem, P.D. Nunn, A.J. Payne, W.T. Pfeffer, D. Stammer and A.S. Unnikrishnan, Sea Level Change. In*: Climate Change 2013: The Physical Science Basis. Contribution of Working Group I to the Fifth Assessment Report of the Intergovernmental Panel on Climate Change* [Stocker, T.F., D. Qin, G.-K. Plattner, M. Tignor, S.K. Allen, J. Boschung, A. Nauels, Y. Xia, V. Bex and P.M. Midgley (eds.)]. Cambridge University Press, Cambridge, United Kingdom and New York, NY, USA, (2013)

[6] Orlić M., *Mala internet škola oceanografije – Uspori u Jadranu*, URL: http://skola.gfz.hr/d1_8.htm (2.5.2021.)

[7] BBC, *Venice floods: Climate change behind highest tide in 50 years, says mayor*, URL: https://ichef.bbci.co.uk/news/976/cpsprodpb/1461C/production/_109648438_hi057966143.jpg (29.3.2021)

[8] Orlić M., *Mala internet škola oceanografije – Plimne oscilacije u Jadranu*, URL: http://skola.gfz.hr/d1_7.htm (27.3.2021)

[9] Polli, S., *La propagazione delle maree nell'Adriatico*, IX Convegno della Associazione Geofisica Italiana, Associazione Geofisica Italiana, Roma, 1-11 (1959)

[10] Monserrat, S., Vilibić, I., Rabinovich A.B., *Meteotsunamis: atmospherically induced destructive ocean waves in the tsunami frequency band*, Natural Hazards and Earth System Sciences, **6**, 1035-1051 (2006)

[11] Vilibić, I., Šepić, J., *Destructive meteotsunamis along the eastern Adriatic coast: Overview*, J. Phys. Chem. Earth, **34**, 904-917 doi: *10.1016/j.pce.2009.08.004* (2009)

[12] Dalmatinski portal, *Prije 40 godina meteorološki tsunami poharao je Vela Luku*, URL: https://dalmatinskiportal.hr/sadrzaj/fotografije/2018-06-21-17-43-563043870/964547657-936664389-639069781.jpg (29.3.2021)

[13] *Data from automatic measuring systems of Institute of Oceanography and Fisheries, Split, Croatia*, URL: http://faust.izor.hr/autodatapub/mjesustdohvatpod?jezik=eng (5.8.2020)

[14] Copernicus Climate Change Service (C3S): *ERA5: Fifth generation of ECMWF atmospheric reanalyses of the global climate,* Copernicus Climate Change Service Climate Data Store (CDS), URL: https://cds.climate.copernicus.eu/cdsapp#!/home (13.1.2021)

[15] Pawlowicz, R., Beardsley, B., Lentz, S., *Classical tidal harmonic analysis including error estimates in MATLAB using T_TIDE,* Computers & Geosciences, **28**, 929-937 (2002)

[16] Walker, J., Halliday, D., Resnick, R., *Fundamentals of physics. Hoboken*, NJ: Wiley (2011)

[17] Vilibić, I., N. Domijan, M. Orlić, N. Leder, M. Pasarić, *Resonant coupling of a traveling air pressure disturbance with the east Adriatic coastal waters*, J. Geophys. Res., **109**, doi:*10.1029/2004JC002279* (2004)

[18] Orlić, M., *Mala internet škola oceanografije – Uspori*, URL: http://skola.gfz.hr/d1_2.htm (13.7.2021)